ELSEVIER

Journal of Organometallic Chemistry 655 (2002) 70–88

Journal of Organo metallic Chemistry

www.elsevier.com/locate/jorganchem

Chiral organometallic chromophores for nonlinear optics derived from $[Fe_2(\eta^5\text{-}C_5H_5)_2(CO)_2(\mu\text{-}CO)(\mu\text{-}C\text{–}CH_3)]^+$ $[BF_4]^-$

Richard D.A. Hudson [a], Anthony R. Manning [a,*], John F. Gallagher [b,*], Marie Helena Garcia [c], Nelson Lopes [c], Inge Asselberghs [d], Roel Van Boxel [d], André Persoons [d], Alan J. Lough [e]

[a] Department of Chemistry, University College Dublin, Belfield, Dublin 4, Ireland
[b] School of Chemical Sciences, Dublin City University, Dublin 9, Ireland
[c] Complexo 1, IST, Av. Rovisco Pais, 1049-001 Lisboa Codex, Portugal
[d] Katholieke Universiteit Leuven, Celestijnenlaan 200D, B3001 Leuven, Belgium
[e] Department of Chemistry, University of Toronto, Toronto, ON, Canada MS5 3H6

Received 12 March 2002; accepted 20 March 2002

Abstract

Two series of chiral organometallic Donor-π-Acceptor chromophores derived from $[Fe_2(\eta^5\text{-}C_5H_5)_2(CO)_2(\mu\text{-}CO)(\mu\text{-}C\text{–}CH_3)]^+$ $[BF_4]^-$ have been synthesised. In the first series (*S*)-(−)-2-methoxymethyl pyrrolidine acts as the chiral donor end group and in the second series 1,1′-binaphthyl acts as the chiral π-bridging unit. The nonlinear optical properties of these compounds were measured by the Kurtz powder technique and by hyper-Raleigh scattering. β-values of up to 964×10^{-30} esu were obtained for a member of the first series. Single crystal X-ray studies of $[Fe_2(\eta^5\text{-}C_5H_5)_2(CO)_2(\mu\text{-}CO)(\mu\text{-}C\text{–}CH_3)]^+$ $[BF_4]^-$, $[Fe_2(\eta^5\text{-}C_5H_4CH_3)_2(CO)_2(\mu\text{-}CO)(\mu\text{-}(E)\text{-}C\text{–}CH{=}CH\text{-}2\text{-}(5\text{-piperidin-1-yl-thiophene}))]^+$ $[BF_4]^-$ and $[Fe_2(\eta^5\text{-}C_5H_4CH_3)_2(CO)_2(\mu\text{-}CO)(\mu\text{-}(E)\text{-}C\text{–}CH{=}CH\text{-}2\text{-}(\text{naphthalene}))]^+$ $[BF_4]^-$ are reported.

Keywords: Nonlinear optics; Kurtz powder; Hyper-Raleigh scattering; Second harmonic generation; Iron; Crystal structures

1. Introduction

Organometallic groups are receiving considerable attention in nonlinear optical (NLO) studies due to the flexible nature of their substitution and oxidation states [1]. They have been utilised as donors (D) or acceptors (A) in the well established D-π-A motif, and very high hyperpolarisabilities (β-values) have been obtained by the judicious combination of bridging element and end groups [2]. In this context we are interested in the cationic complex $[Fe_2(\eta^5\text{-}C_5H_5)_2(CO)_2(\mu\text{-}CO)(\mu\text{-}C\text{–}CH_3)]^+$ $[BF_4]^-$ (**1**), (originally synthesised by Rosenblum and co-workers [3]), which may function as an acceptor end group after facile condensation with aldehydes to form diiron alkenylidyne complexes [4] (Scheme 1).

A theoretical study has revealed that the cationic μ-carbyne may efficiently accept electron density into the formally vacant π-orbital from an adjacent donor throughout rotation about the μ-C–C=CHR single bond [5]. Research by Green and co-workers has shown that derivatives of **1** may have potential for 2nd order NLO studies [6]. We have recently sought to extend this work by synthesising a number of merocyanine structures incorporating this acceptor and subsequent measurements by hyper-Raleigh scattering (HRS) [7] have shown that some of these compounds exhibit extremely high β-values [8]. HRS is measured in solution and since β is a vector quantity; in centrosymmetric environments all of its components disappear. Therefore, for measurements in the solid state, compounds that crystallise in an acentric space group are desirable [9]. This was well illustrated in a ground-breaking report by Green et al., in which they observed (by the Kurtz powder technique

* Corresponding authors. Tel.: +353-1-7045114; fax: +353-1-7045503.
E-mail addresses: anthony.manning@ucd.ie (A.R. Manning), john.gallagher@dcu.ie (J.F. Gallagher).

0022-328X/02/$ - see front matter
PII: S0022-328X(02)01415-8

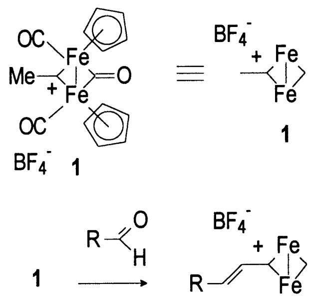

Scheme 1. **1**; ($[Fe_2(\eta^5\text{-}C_5H_5)_2(CO)_2(\mu\text{-}CO)(\mu\text{-}C\text{–}CH_3)]^+$ $[BF_4]^-$).

[10]) that (*Z*)-[1-ferrocenyl-2-(4-nitrophenyl)-ethylene] exhibits a large second harmonic generation (SHG) powder efficiency (62 × urea), whereas the *E*-isomer is completely inactive in the solid state despite its larger molecular hyperpolarisability [11]. This was attributed to the acentric crystal packing of the *Z*-isomer as opposed to the presumed centrosymmetric space group, which the *E*-isomer resided in. Green's initial observation of the *p*-dimethylaminophenylethenyl derivative of **1** was also made using the Kurtz powder technique [10]. It is thus remarkable that any SHG signal at all was observed since a crystallographic study of the chromophore reveals that the structure occupies the centrosymmetric space group $P2_1/n$. The powder efficiencies of the compound (0.77 and 3.6 times that of urea, as their $[BF_4]^-$ and $[CF_3SO_3]^-$ salts, respectively) were attributed to either surface effects or to minute crystallographically undetectable deviations from centrosymmetry. It was subsequently recognised that the planar chirality of 1,2-disubstituted and related ferrocenes could also be exploited to promote noncentrosymmetric crystal packing and several groups have reported chromophores derived from this motif [12] with powder efficiencies as high as 220 times that of urea [13]. We have been motivated by these results to introduce chirality into potential NLO candidates derived from **1** and we report here the synthesis and optical measurements of the first generation of this class of chiral organometallic chromophores.

2. Results and discussion

Two series of chiral compounds were synthesised which included an aldehyde functionality in the starting materials for condensation with **1** (Scheme 1) [4]. In the first series the chirality was achieved by the incorporation of a chiral donor (derived from the amine (*S*)-(−)-2-methoxymethyl pyrrolidine [14]) and in the second it arises as a consequence of the inclusion of chiral 1,1′-binaphthyl spacer elements.

2.1. Synthesis of the chiral donor-containing merocyanines *6* and *7*

Thiophenes have been used extensively as conduits for electron transfer in conducting polymers [15] and are effective spacer elements in NLO active materials [8,14c,16]; consequently we have included a thienyl residue in both series of chromophores as part of the π-bridging systems. Aldehydes **2** were readily synthesised according to the method of Prim et al. [17] and these compounds were further homologated to the (*E*)-vinyl aldehydes **3**. Both achiral (**2a**, **3a**) and chiral versions (**2b**, **3b**) of the chromophores were prepared with piperidine and (*S*)-(−)-2-methoxymethylpyrrolidine functioning as the donor end groups, respectively. Optical rotation measurements on the chiral adducts **2b** and **3b** show rotations of $[\alpha]^{Hg}_{546}$: −178 and −155°, respectively. Compound **2a** was further homologated by Horner–Wittig condensation with diethyl(2-thienylmethyl)phosphonate [18] to afford **4** (not shown) followed by formylation to give **5** (Scheme 2).

Condensation of **2** and **3** with **1** in refluxing dichloromethane provided the merocyanines **6** and **7** in reasonable yields as dark red and blue, air-stable solids, respectively, which exhibited the expected spectroscopic and constitutional data. The solids crystallise with fractional amounts of dichloromethane, which is seen in the ^{1}H-NMR and X-ray structure of **9**, vide infra (Scheme 3). As **6** and **7** are highly coloured, reliable optical rotations could not be recorded even at high dilutions and a variety of wavelengths. Unfortunately, **1** did not undergo a condensation reaction with **5** even with prolonged reaction times (5 days) or on the addition of $HBF_4{\cdot}OEt_2$. Instead, **1** was deprotonated to the neutral vinylidene complex **1a** (Scheme 4). This may be attributed to the increasing basicity of the

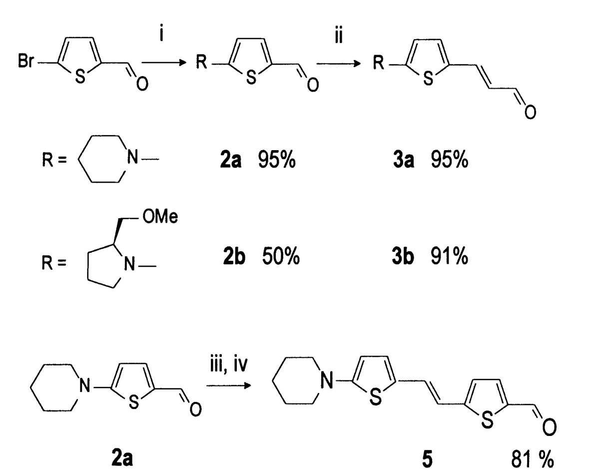

Scheme 2. *Reagents and conditions:* (i) Amine, water, reflux 12 h; (ii) 2-tributylphosphoniumacetaldehyde diethylacetal bromide, THF, KO^{t}Bu, 12 h; (iii) diethyl(2-thienylmethyl)phosphonate, THF, KO^t-Bu, 12 h; (iv) BuLi, DMF, THF.

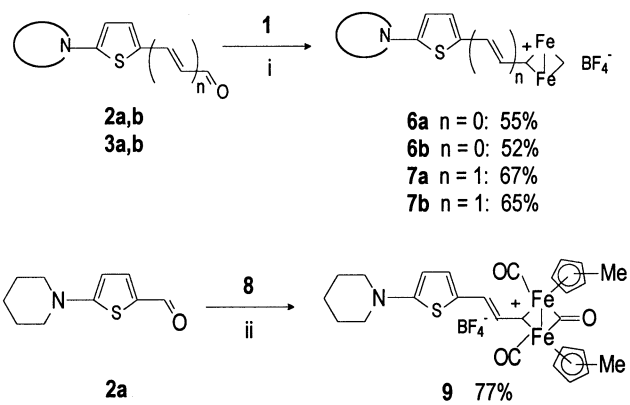

Scheme 3. *Reagents and conditions:* (i) CH_2Cl_2, reflux, 12 h; (ii) $HBF_4{\cdot}OEt_2$, CH_2Cl_2, reflux, 4 h.

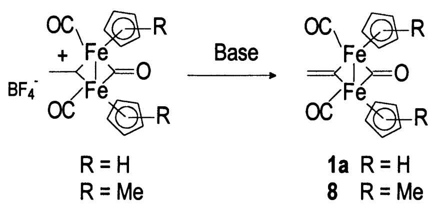

Scheme 4. Formation of the neutral vinylidene complexes **1a** and **8**.

nitrogen atom as the aldehyde functionality is displaced away by longer conjugated path lengths. To a lesser extent this effect was also observed in the condensation times and IR profiles of the successful reactions which produced **6** and **7**. Compounds **3**, having an extra double bond with respect to **2**, took much longer to condense with **1** and appreciable amounts of **1a** were seen in the IR spectra of the reaction mixtures. This slowly diminished as complexes **7** were formed. No evidence of **1a** was detected in the reaction of **2** with **1**.

Neither **6** nor **7** yielded X-ray quality crystals and in order to address the relative insolubility of these compounds and hence their poor crystallisation properties, condensation of the methylcyclopentadienyl analogue of **1**, $[Fe_2(\eta^5\text{-}C_5H_4Me)_2(CO)_2(\mu\text{-}CO)(\mu\text{-}C\text{–}CH_3)]^+$ $[BF_4]^-$ (**8**) (Scheme 4), with **2a** was attempted. This salt is much less reactive than **1** towards condensation with aldehydes and would not react with the relatively deactivated aldehyde in **2a**. However, reaction of **2a** with the neutral species **8** in the presence of $HBF_4{\cdot}OEt_2$ afforded **9** from which X-ray quality crystals were obtained (Fig. 3, vide infra). Condensation of **8** with chiral **2b** was very slow and only decomposition products were obtained. Representative spectroscopic data for compounds **6**, **7** and **9** are collected in Table 1.

2.2. *Synthesis of the naphthyl and chiral 1,1′-binaphthyl-containing merocyanines* ***13, 14, 15, 19, 22, 23*** *and* ***26***

In the case of all of the naphthyl-bridged merocyanines described below we chose to use methoxy groups as the donor moieties, and where possible, to arrange the end groups of the chromophores in a 2,3- (the shortest distance) or 2,6- (the longest distance) relationship about the naphthylene spacer. The 1,1′-binaphthyl motif incorporating alkoxy donors has been examined in this latter configuration by other investigators both in the racemic [19] and resolved forms [20] for NLO activity.

In order to examine the efficiency of the methoxy group as a donor in either of these configurations the model compounds **13**–**15** were synthesised from the readily accessible aldehydes **10**–**12** by condensation with **1** in a manner analogous to the synthesis of **6** and **7** (Scheme 5). These complexes were obtained as red–brown solids and exhibited all the expected spectroscopic and constitutional data. A single crystal was grown of **15** and the structure was established by X-ray diffraction (Fig. 4).

Racemic 1,1′-bi-2-naphthol was prepared according to the literature procedure [21] and resolved according to the method of Cai et al. [22]. The racemate and enantiomers were methylated to afford 2,2′-dimethoxy-1,1′-binaphthyl and formylated by *ortho*-metallation followed by a DMF quench. During the course of this reaction we obtained the *ortho*-monoaldehydes **16** (*R*/*S* and racemate; from (*R*)-1,1′-bi-2-naphthol $[\alpha]_D$: + 101.6°; from (*S*)-1,1′-bi-2-naphthol $[\alpha]_D$: −100.4°) and the dialdehydes **20**. Compound **16** was converted [18] to the monoaldehydes **17** (*R*/*S* and racemate: from (*R*)-1,1′-bi-2-naphthol $[\alpha]_D$: +221.1°; from (*S*)-1,1′-bi-2-naphthol $[\alpha]_D$: −222.9°). Both **16** and **17** condensed with **1** to give **18** (*R*/*S* and racemate) and **19** (*R*/*S* and racemate) (Scheme 6). These were isolated as red/brown and blue solids, respectively, which exhibited all the expected spectroscopic and constitutional data (Scheme 6).

The dialdehydes **20b** (*R*/*S* and racemate) were prepared from 6,6′-dibromo-2,2′-dimethoxy-1,1′-binaphthalene by double halogen–metal exchange with *n*-butyl lithium followed by a DMF quench. Both **20a** (*R*/*S* and racemate, see above) and **20b** (*R*/*S* and racemate) were condensed with **1** to afford chromophores **21** (*R*/*S* and racemate) and **22** (*R*/*S* and racemate) (Scheme 7), which were recovered as brown/red solids. Unfortunately, both were highly insoluble and ^{13}C-NMR spectroscopic data could not be recorded. However, all the other data required for unambiguous characterisation were obtained. Chain extension of both aldehydes in **20b** (*R*/*S* and racemate) with the Wittig reagent diethyl(2-thienylmethyl)phosphonate afforded 2,2′-dimethoxy-6,6′-bis(*E*-2-(2-thiophene))ethenyl)-1,1′-binaphthalene, (**24**) (*R*/*S* and racemate) (not shown) which were formylated to **25** (enriched *R*/*S* and racemate). Some scrambling of the enantiomers occurred in the conversion of **20b** to **25** (optical rotation data: from *R*-1,1′-binaphthyl:

Table 1
Selected spectroscopic data for compounds **6**, **7**, **9**, **13**, **14**, **15**, **18**, **19**, **21**, **22** and **26**

Entry	Compound	λ_{max} [a] (nm) ($\varepsilon \times 10^3$, M^{-1} cm^{-1})			ν_{CO} [b] (cm^{-1})	δ $\mu^{13}C$ [c] (ppm)
		CH_2Cl_2	CH_3CN	ΔE/kJ M^{-1}		
1	**1**	–	–		2047, 2016, 1853	499
2	**1a**	528 (1)	528 (1)	0	1992, 1953, 1790	272
3	**6a**	557 (80)	547 (68)	4	2013, 1982, 1820	349
4	**6b**	556 (57)	547 (52)	3	2014, 1981, 1821	350
5	**9**	562 (59)	551 (53)	5	2008, 1976, 1816	354
6	**7a**	658 (86)	643 (60)	4	2009, 1980, 1815	340
7	**7b**	655 (97)	640 (73)	5	2010, 1983, 1816	340
8	**13**	467 (27)	441 (26)	15	2035, 2002, 1845	441
9	**14**	458 (49)	448 (58)	4	2033, 2004, 1843	438
10	**15**	511 (61)	481 (49)	14	2034, 2005, 1844	432
11	**18**	460 (23)	451 (22)	5	2036, 2005, 1846	437
12	**19**	608 (62)	566 (58)	15	2032, 2002, 1841	417
13	**21**	453 (–)	446 (–)	4	2034, 1992, 1844	–
14	**22**	523 (52)	496 (53)	13	2034, 2007, 1842	–
15	**26**	633 (75)	594 (75)	12	2031, 2000, 1840	416

[a] Measured at 1×10^{-5} mol.
[b] Recorded in CH_2Cl_2.
[c] Recorded in CD_2Cl_2.

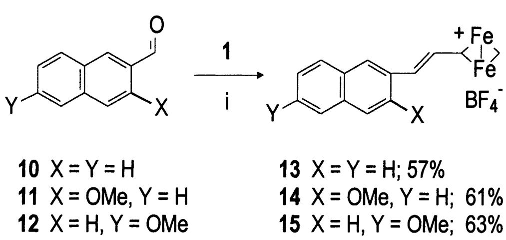

Scheme 5. *Reagents and conditions:* (i) CH_2Cl_2, reflux, 12 h.

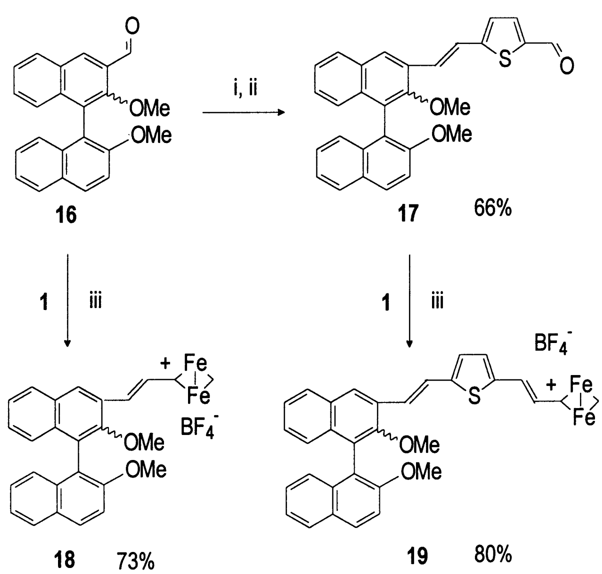

Scheme 6. *Reagents and conditions:* (i) Diethyl(2-thienylmethyl)phosphonate, KO^{t}Bu, THF, 1 h; (ii) BuLi, THF, −78 °C, 1 h. DMF, 30 min; (iii) CH_2Cl_2, reflux 18 h.

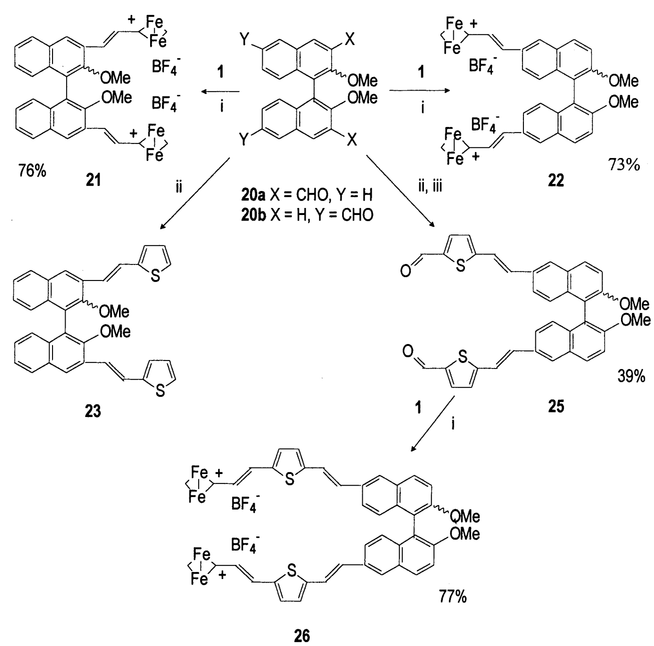

Scheme 7. *Reagents and conditions:* (i) CH_2Cl_2, reflux 18 h; (ii) diethyl(2-thienylmethyl)phosphonate, KO^{t}Bu, THF, 1 h; (iii) BuLi, THF, −78 °C, 1 h. DMF, 30 min.

$[\alpha]_D$: −650.2° and from *S*-1,1′-binaphthyl: $[\alpha]_D$: + 569.1°). Compound **25** condensed with **1** giving **26** (enriched *R*/*S* and racemate) in good yield as red solids (Scheme 7). Unfortunately, although **20a** (racemate) reacted with diethyl(2-thienylmethyl)phosphonate, the product, **23** (racemate), was too insoluble to allow further study. Representative spectroscopic data for compounds **13**, **14**, **15** and racemic **18**, **19**, **21**, **22**, and **26** are collected in Table 1.

2.3. Linear optical and NMR properties of **6**, **7**, **9**, **13**, **14**, **15**, **18**, **19**, **21**, **22** and **26**

The spectroscopic data for compounds containing the six-membered piperidine donor, **6a**, **7a** and **9**, differ little from those for compounds containing the five-membered pyrrolidine residue, **6b** and **7b** (Table 1). Inclusion of the pendant functionality in **7**, in order to induce asymmetry in the solid state, appears to have no linear spectroscopic effect in solution. Compounds **6** are dark red solids and have UV–vis absorbances at 557 and 556 nm in dichloromethane. These bands are attributable to donor–acceptor based charge transfer (CT) on photochemical excitation from the ground to excited state. The position of the CT bands is unfortunate since the laser frequency used for the Kurtz powder measurements is 1064 nm and so any second harmonic signal at 532 nm would fall directly in this range and be absorbed. Increasing the π-spacer in a D-π-A chromophore results in a shift to lower energies of the principle absorption band and this was the initial motivation for the synthesis of **5** and its condensation product with **1**. As **5** did not condense, compounds **7** were synthesised and it was found that the extra double bond was enough to bathochromically shift the CT band away from the region of interest at 532 to around 640 nm.

Chromophores **13**, **14**, **15**, **18**, **19**, **21**, **22** and **26** are dark brown to blue solids and have absorbances in the range 421 (for **13** in acetonitrile) to 633 nm (for **26** in CH_2Cl_2). The higher energies of their CT transitions suggest that their donor–acceptor interactions are weaker than they are for **6** and **7**. This might have been expected from the Hammett parameters σ_p $NMe_2 = -0.63$ and σ_p OMe $= -0.28$ [23]. Comparison of **13**, in which there is no methoxy substituent, with **15** and **22** suggests that in the 2,6-substitution pattern the methoxy group acts as a moderate donor. The lowering of the ν_{CO} frequencies and the upfield shift of the $^{13}C_{\mu}$ resonance of the $Fe_2(\eta^5\text{-}C_5H_5)_2(CO)_2(\mu\text{-}CO)(\mu\text{-}C\text{–})$ end group suggests that in the ground state its positive charge is delocalised onto the methoxy group as well as the naphthyl spacer. There is a consequent lowering of the energy of the CT transition in going from **13** to **15**. Its further lowering in **22** suggests that there is some interaction between the two methoxynaphthyl subunits.

In contrast the presence of an *ortho*-MeO group appears to hinder the communication between the $Fe_2(\eta^5\text{-}C_5H_5)_2(CO)_2(\mu\text{-}CO)(\mu\text{-}C\text{–})$ end group and the naphthyl part of the spacer. This is particularly apparent in the $^{13}C_{\mu}$ chemical shifts and the energies of the CT transitions. The former are more downfield for the 2,3-derivatives than the 2,6- and are not very different from the values for **13**, whilst the latter are of higher energies for **14**, **18** and **21** than for **15** and **22**, and are even higher than for **13**. A possible explanation is that steric interaction between the *ortho*-methoxy group and the –CH=CH– moiety causes rotation about the C–naphthyl bond and reduces the p_π–p_π overlap between aromatic ring and CC double bond. However, it may be that the methoxy group in this *ortho*-arrangement is simply not acting as donor (σ_o OMe = 0.10 [23]).

The two level model [24] predicts that the dipole moment change on excitation is important in SHG and insight into this process may be gained from the solvatochromic behaviour of the compounds [25]. Both series of chromophores exhibit λ_{max} values that are solvent dependent. For derivatives **6** and **7** this dependency is small with around 4 kJ M^{-1} but for some of the naphthyl-containing merocyanines the energy differences are more significant. The expected decrease in energy on excitation of **14** versus **15** commensurate with the increase in length of the chromophores and the more effective donor–acceptor arrangement is accompanied by an increase in solvatochromism with **14** ($\Delta E = 4$ kJ M^{-1}) apparently exhibiting a smaller dipole moment change than **15** ($\Delta E = 14$ kJ M^{-1}). Unsurprisingly a similar ΔE value of 4–5 kJ M^{-1} is observed for both **14** and **18** on elaboration of the bridging unit to the 1,1′-binaphthyl core but this is accompanied by an unexpected decrease in extinction coefficient of around 26 000 M^{-1} cm^{-1} (CH_2Cl_2). Similar solvatochromic behaviour is manifested between **21** ($\Delta\lambda = 4$ kJ M^{-1}) and **22** ($\Delta\lambda = 13$ kJ M^{-1}). These full binary chromophores also appear to suffer a loss in extinction coefficient in comparison with their naphthyl counterparts **14** and **15**. They may be expected to exhibit ε values twice that of **14** and **15** but the value obtained for **22** is comparable to **15**. The large decrease in excitation energy and apparent increased dipole moment change between **18** ($\Delta E = 5$ kJ M^{-1}) and **19** ($\Delta E = 15$ kJ M^{-1}) is probably due to the auxiliary donor effect of the electron-rich thiophene ring which compensates for the lack of communication between the putative out-of-plane acceptor and the poorly donating *ortho*-methoxy group.

The ^{13}C-NMR chemical shift for the cationic μ-carbyne is indicative of the amount of charge residing on the diiron moiety. The μ-carbyne in **1** has an extremely low field chemical shift of δ 499 and compounds **6** and **7** have shifts about 150 ppm upfield of this at around δ 350 and 340, respectively (Table 1). It is informative to compare these values with those obtained for **1a**, which is comparable to the diiron fragment in the limiting CT resonance forms of **6** and **7** on excitation. Compound **1a** exhibits a neutral μ-carbene shift of δ 272, which is about 80 ppm upfield of **6** and **7**. This trend also appears in the IR data with ν_{CO} stretches around 30 cm^{-1} higher for **1** than **6** and **7**, which indicates increased M–CO back donation. These are in turn around 20 cm^{-1} above the ν_{CO} stretches for the neutral **1a**. The extra double bond in compounds **7** with respect to **6** contributes more resonance canonical

Table 2
Comparison of dimensions of **1** with those of related [$Fe_2(\eta^5$-$C_5H_5)_2(CO)_2(\mu$-$CO)(\mu$-$CX)$] compounds (Å and °)

Compound	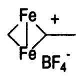	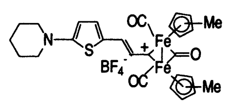	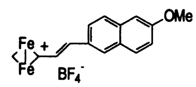	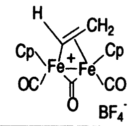	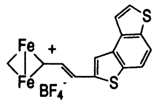	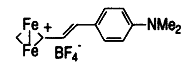	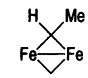
Number	**1**[a]	**9**	**15**	**27**[34]	**28**[8b]	**29**[6]	**30**[34]
	Cation	Cation	Cation	Cation	Cation	Cation	Neutral
Fe-Fe/Å	2.499(3)/ 2.503(3)	2.4995(11)	2.5105(14)	2.595(2)	2.508(1)	2.505(1)	2.520(2)
Fe-C_O/Å	1.95	1.902(7)/1.915(6)	1.924(7)/1.941(7)	1.963(8)	1.936(7)	1.921(5)/1.941(5)	1.903(3)
Fe-C_C/Å	1.84	1.877(5)/1.878(5)	1.847(6)	1.980(8)	1.831(1)/1.836(6)	1.861(5)/1.895(5)	1.986(3)
C_C-C/Å	1.43	1.365(6)	1.400(9)	1.40(2)	1.416(7)	1.373(7)	1.514(5)
Fe-C_O-Fe/°	79.6	81.8(3)	81.0(3)	82.7(4)	80.2(3)	80.9(2)	82.9(2)
Fe-C_C-Fe/°	85.7	83.5(2)	85.8(3)	81.8(4)	86.3(2)	84.5(2)	78.8(1)
Fe-C-O/°	140.2	139.9(5)/138.2(5)	138.9(6)/140.1(6)	138.6(2)	140.1(6)/139.5(6)	141.0(4)/138.1(4)	138.5(1)
Fe-C-C/°	137.1	137.8(4)/138.6(4)	134.1(5)/140.1(5)	128.4(10)	134.9(4)/138.6(4)	134.6(4)/140.9(4)	123.7(2)

[a] Mean values are recorded for lengths and angles.

forms to the overall description of the charge-separated states and so lower μ-carbyne and ν_{CO} values are recorded for these complexes. These spectroscopic findings suggest that the complexes are extensively delocalised with, in effect, almost two-thirds of the positive charge residing on the organic ligand.

The ground state structure in **6**, **7** and **9** may be regarded as a mixture of canonical forms, the limiting forms of which for **6b** are shown in Fig. 1. In one, **A/B**, the positive charge resides on the bridging carbon atom of the diiron end group, but in the other **A1/B1** it resides on N and there is an iminium contribution. In the examples where there is a substituent adjacent to the nitrogen (**6b** and **7b**) there is the potential to use NMR spectroscopy to observe restricted rotation about the nitrogen–thiophene bond since **A1** and **B1** are different configurational isomers.

Low temperature NMR studies on **6b** and **7b** show that the thienyl proton adjacent to the nitrogen-containing ring has a coalescence temperature of 24 and 7 °C in **6b** and **7b**, respectively, corresponding to rotational barriers about the *N*-thiophene single bond of around 14.3 and 12.4 kcal mol^{-1}. As expected, the energy barrier for **7b** is the lower of the two due to the larger

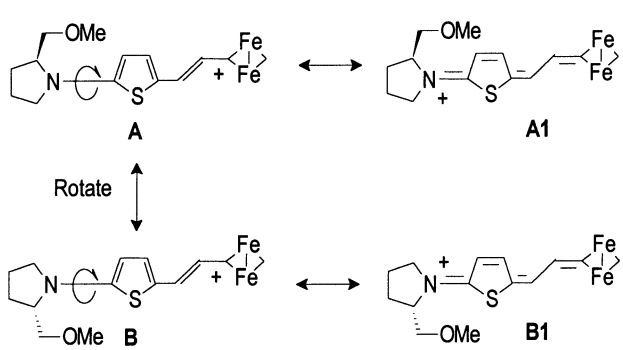

Fig. 1. Limiting canonical forms contributing to the presence of rotational barriers in **6b**.

number of accessible canonical forms for charge delocalisation over the longer bridge. Although rotation about the C–C bonds between vinyl and divinyl linkages to C_μ might also be expected to be restricted, we were unable to investigate them at the temperatures available to us (ca. −30 °C). Casey et al. have studied the rotational barriers of several cationic diiron μ-carbyne complexes at temperatures as low as −103 °C as this is often necessary to slow down rotations in alkyl and alkoxy substituted merocyanines. They concluded that the barrier to rotation about the carbyne carbon to vinyl carbon bond is very low and can only be observed when a good electron donor is attached to the remote vinyl carbon [5]. For example, in the case of the dimethylaminovinyl complex [$Fe_2(\eta^5$-$C_5H_5)_2(CO)_2(\mu$-$CO)(\mu$-C–CH=CH–$NMe_2)$][BF_4] the C_μ-to-vinyl rotational barrier is 19.8 kcal mol^{-1} with coalescence at 93 °C [5]. This is reduced to 10.6 kcal mol^{-1} (observed at −73 °C) in [$Fe_2(\eta^5$-$C_5H_5)_2(CO)_2(\mu$-$CO)(\mu$-C–CH=CH–C_6H_4–NMe_2-4)][BF_4] (**29**, Table 2) where a phenyl group intervenes between the donor and the acceptor; the barrier to rotation about the phenyl–vinyl bond was 13.0 kcal mol^{-1} [5]. From line width analysis a rate of exchange for rotation about the carbon nitrogen bond in the former complex was estimated to be >22.7 and 10.9 kcal mol^{-1} in the latter. In our compounds the amine donors are separated from the diiron moiety by ethenylthiophene linkages and the barriers to rotation (14.3 and 12.4 kcal mol^{-1}, respectively) should be slightly greater than that observed for [$Fe_2(\eta^5$-$C_5H_5)_2(CO)_2(\mu$-$CO)(\mu$-C–CH=CH–C_6H_4–NMe_2-4)][BF_4] (10.9 kcal mol^{-1}) due to the higher resonance energy of benzene versus thiophene. Conversely they should be much lower than that observed for [$Fe_2(\eta^5$-$C_5H_5)_2(CO)_2(\mu$-$CO)(\mu$-C–CH=CH–$NMe_2)$][BF_4] (22.7 kcal mol^{-1}) as the nitrogen is separated from the cationic centre by the extra distance and aromaticity of the intervening thiophene. Indeed, the spectroscopic data discussed above support these assumptions.

Compounds **13**, **14**, **15**, **18**, **19** and **26** exhibit cationic μ-carbyne resonances much closer to the δ 499 shift for **1** indicating less delocalisation of charge throughout the structures as expected, nonetheless the trends identified in the UV spectroscopic data are still evident. The 2,3-substituted series **14** and **18** (Table 1) exhibit shifts at δ 438 and 437 (compound **21** was too insoluble to measure) comparable to **13** at δ 441 and these values decrease to around δ 432 in the 2,6-substituted compound **15**. For the lengthier **19** and **26** a more upfield shift to around at δ 417 was recorded. No rotational barriers for any of the compounds in this series could be observed at the temperatures accessible to us. The IR data also support these observations with a general decrease in stretching frequency for this series with respect to **1** although this is not as marked as in the more highly delocalised compounds **6**, **7** and **9** (Table 1).

2.4. X-ray structures of *1, 9 and 15*

There are now several structures for adducts of **1** in the literature [4–6,26] but there has been no diffraction study of the paradigm compound **1** despite the fact that it has been known for over 20 years [3]. Clearly it would be relevant to have a structure for the parent complex with which to compare the bond lengths and angles within the diiron core with those of the more delocalised vinylogous adducts and we have sought to obtain one. Compound **1** is insoluble in many common polar organic solvents and often undergoes deprotonation in solution rendering it difficult to crystallise in the normal way (diffusion or layering of ethereal solvents over polar solutions of the salt) and so we undertook a different approach. Compound **1** was deliberately deprotonated to form its conjugate base **1a**, which was dissolved in a small amount of diethyl ether. This was placed in a narrow test tube and more diethyl ether was carefully added so two layers were formed. Several drops of $HBF_4 \cdot OEt_2$ (54% solution in diethyl ether) were introduced into the upper layer and the solution allowed to stand overnight. An X-ray diffraction study of the poor quality fine needles formed by this method provided a structure for **1**.

Although the crystals of **1**, **9** and **15** only diffracted relatively poorly (see Table 3 for details of crystal data and structure refinement) we were able to obtain sufficient data to allow us to determine the details of their conformations unequivocally. For the structures of **9** and **15**, important information was obtained on relevant parameters with a reasonable precision. Selected data for **1**, **9** and **15** are tabulated in Table 2 along with some closely related structures for comparative purposes.

Interestingly **1** was found to have crystallised in the orthorhombic acentric space group $P2_1nb$ (Table 3) with two anions and two cations in the asymmetric unit. An ORTEP view of one of the cations, from molecule B, is depicted as Fig. 2, and selected bond lengths and angles are given in Table 2. In **1** the core geometry of the two independent cations of $[Fe_2(\eta^5\text{-}C_5H_5)_2(CO)_2(\mu\text{-}CO)(\mu\text{-}C{-}CH_3)]^+$ are essentially identical with Fe–Fe bond lengths of 2.499(3) and 2.503(3) Å for the A and B molecules, respectively. There is some disorder in the structure of **1**, principally with respect to the $[BF_4]^-$ anions. The four Fe–$CO_{terminal}$ bond lengths are in the range 1.73(2)–1.80(2) Å and Fe–CO angles are close to linearity as expected 177(2)°. The four $CO_{terminal}$ distances are normal and lie in the range 1.11–1.18(2) Å. The bridging μ(C–CH_3) ligand has Fe–C distances from 1.818(18) to 1.862(16) Å, with C–CH_3 bond lengths of 1.42(3) and 1.45(3) Å. This contrasts with the μ(CO) moiety where the Fe–C distances are in the range 1.93(2)–1.96(2) Å and C–O bond lengths are 1.14(2) Å. The Fe–C_O–Fe bond angles are 79.1(9)/80.1(7)° in contrast to 85.3(7)/86.1(8)° for the bridging CCH_3 in Fe–C_C–Fe. The Fe–$CO_{bridging}$ angles are in the range from 138.8(15) to 141.2(19)° and the Fe–C–CH_3 angle is between 136.3(15) and 137.9(15)°, with little difference between the two sets of angles. The terminal carbonyl ligands are eclipsed with respect to one another with 2.2(5)° for O1A···Fe1A–Fe2A···O2A and −1.5(5)° for O1B···Fe1B–Fe2B···O2B, likewise the η^5-C_5H_5 rings (with Cg1···Fe1A–Fe2A···Cg(2) = 1.9(7)° and Cg3···Fe1B–Fe2B···Cg4 = 1.4(8)°) are eclipsed and *cis*- with respect to one another (Cg1, Cg2, Cg3, Cg4 are the four cyclopentadienyl ring centroids on molecules A and B). The two tetrafluoroborate anions are disordered and were both modelled with two different site orientations and restrained bond length and angle DFIX controls in the full matrix least-square refinements cycles. There are no classical hydrogen bonds in the crystal structure although there are numerous C–H···F contacts.

The structure of the ruthenium analogue of **1** has been determined previously [27]. Unlike **1**, this structure crystallises in a centrosymmetric space group, monoclinic $P2_1/n$ and has been determined to a high degree of precision. The structure is similar to the two independent molecules A and B in **1**. The C–CH_3 bond length is 1.462(6) A as compared to 1.42(3) and 1.45(3) A in **1**. Of interest is the fact that these two compounds crystallise in different space groups. This may be due to steric and molecular size reasons primarily giving rise to the inability of the iron dimer to crystallise well using well-tried solvent systems, unlike the ruthenium analogue.

The IR spectra of **6**, **7**, **9**, **13**–**15**, **18**, **19**, **21**, **22** and **26** show that both in solution and in the solid state their $Fe_2(\eta^5\text{-}C_5H_5)_2(CO)_2(\mu\text{-}CO)(\mu\text{-}C{-})$ end groups have a

Table 3
Crystal data and structure refinement for **1**, **9** and **15**

Compound	**1**	**9**	**15**
Empirical formula	$C_{15}H_{13}BF_4Fe_2O_3$	$C_{27}H_{28}BF_4Fe_2NO_3S$, $0.49(C_4H_8O)$,$0.53H_2O$	$C_{27}H_{21}BF_4Fe_2O_4$
Formula weight	439.76	694.27	607.95
Temperature (K)	123(2)	295(2)	294(2)
Wavelength (Å)	0.71073	0.71073	0.71073
Crystal system	Orthorhombic	Monoclinic	Monoclinic
Space group	$P2_1nb$	$C2/c$	$P2_1/c$
Unit cell dimensions			
a (Å)	12.697(2)	20.6105(16)	18.239(2)
b (Å)	14.998(2)	16.8844(14)	9.6005(16)
c (Å)	17.232(3)	17.759(3)	14.635(2)
β (°)	–	97.131(9)	93.225(7)
V (Å^3)	3281.5(9)	6132.4(11)	2558.7(7)
Z	8	8	4
D_{calc} (Mg m^{-3})	1.780	1.504	1.578
Absorption coefficient (mm^{-1})	1.821	1.075	1.195
$F(000)$	1760	2856	1232
Crystal size (mm)	0.30 × 0.10 × 0.05	0.60 × 0.17 × 0.10	0.48 × 0.20 × 0.13
θ Range for data collection (°)	2.5–25.0	2.5–26.0	2.2–26.1
Index ranges	$-15 \le h \le 15$, $-17 \le k \le 17$, $-20 \le l \le 20$	$-25 \le h \le 1$, $-1 \le k \le 20$, $-21 \le l \le 21$	$-22 \le h \le 22$, $0 \le k \le 11$, $-18 \le l \le 0$
Reflections collected	5564	6997	7926
Unique reflections	5564	6014	5053
Completeness to $2\theta = 26°$	99%	100%	99%
Max/min transmission	0.91, 0.61	0.900, 0.565	0.86, 0.60
Data/restraints/parameters	5564/305/481	6014/171/514	5053/250/482
Final R indices [$I > 2\sigma(I)$]	$R_1 = 0.149$, $wR_2 = 0.235$	$R_1 = 0.062$, $wR_2 = 0.112$	$R_1 = 0.079$, $wR_2 = 0.188$
R indices (all data)	$R_1 = 0.193$, $wR_2 = 0.254$	$R_1 = 0.164$, $wR_2 = 0.147$	$R_1 = 0.151$, $wR_2 = 0.230$
Goodness-of-fit on F^2	1.225	1.000	1.015
Largest difference peak and hole (e Å^{-3})	0.77/−0.87	0.38/−0.29	0.92/−0.80
Largest shift and error maximum	0.004	0.001	0.001

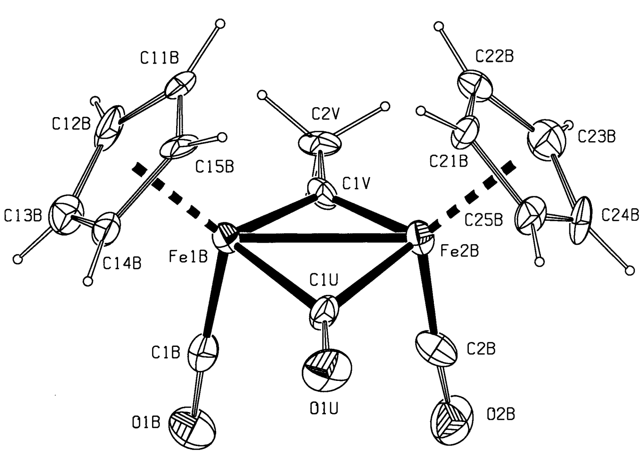

Fig. 2. ORTEP diagram of the major conformation of the iron dimer cation of molecule B in **1**. Displacement ellipsoids are depicted at the 30% level.

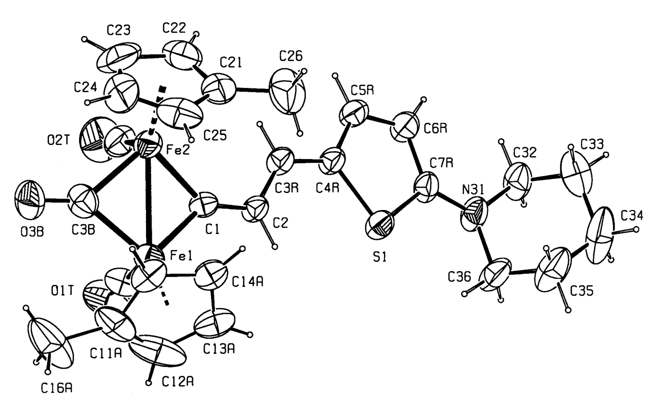

Fig. 3. ORTEP diagram of the major conformation of the iron dimer cation in **9**. Displacement ellipsoids are depicted at the 30% level.

cis conformation comparable to that found in **1** (cf. Ref. [8] for a discussion). This was verified by X-ray diffraction studies of **9** and **15**.

Unlike **1**, **9** crystallises in a centrosymmetric space group (monoclinic, $C2/c$). A representative ORTEP view of the cation is shown in Fig. 3 with selected bond lengths and angles listed in Table 2. The methylcyclopentadienyl ligands show some disorder over two sites for the methyl substituent. The Fe–CO$_{terminal}$ bond lengths are 1.726(7), 1.722(9) Å and the Fe–CO angles are close to linearity 179.1(2)/179.2(2)°; the two terminal CO distances are 1.149(7) and 1.163(8) Å. The bridging μ(C–CH_3) ligand $Fe_{1,2}$–C distances are 1.877(5) and

1.878(5) Å. The suggested highly delocalised ground state structures of **6** and **7** are further confirmed by inspection of the crystal structure of **9**. There is essentially complete delocalisation between C1 and C4 with the single bonds C1–C2 1.365(6) Å and C3–C4 1.372(6) Å similar and shortened from the normal sp^2–sp^2 single bond length (1.48 Å) [28]. The double bond C2–C3 {1.380(7) Å} is lengthened in comparison with a normal sp^2=sp^2 double bond (1.32 Å) [28]. Similarly the C7R–N31 1.330(6) Å bond is considerably reduced in length from a typical sp^2–NR_2 bond (1.38 Å) [28] and is among the shortest known bonds between and amine and an aromatic carbon [29]. For the thiophene ring an increased contribution of the quinoid [30] compared with the aromatic structure [31] is seen {C4R–C5R 1.400(7), C5R–C6R 1.354(7) and C6R–C7R 1.416(7) Å}. In comparison the trends along the formal C–C=C–C chain in the benzothiophene derivative **28** (Table 2) reported by us previously [8b] are more distinct 1.416(7)/1.362(7)/1.419(7) Å and the benzothiophene unit itself has no visible quiniodal character, exhibiting the expected bond lengths and angles for this moiety [31]. The μ(CO) moiety has typical distances with the Fe–C bond lengths of 1.902(7) and 1.915(6) Å and with a bridging CO bond length of 1.181(6) Å. The Fe–C_O–Fe bond angle is 81.8(3)° in contrast to the 83.5(2)° for the bridging μ-CCH(ligand) in Fe–C_C–Fe which is similar to, though not as large as in **1** above. The Fe–$CO_{bridging}$ angles are 138.2(5)/139.9(5)° and the Fe–C–CH_3 angles are 137.8(4)/138.6(4)°.

The μ-$CCHCHC_4H_2NC_5H_{10}$ ligand in **9** lies in a slightly twisted arrangement with respect to the plane defined by the two iron atoms and the bridging carbon atom [dihedral angles Fe1–C1–C2–C3R 169.0(5)°, C1–C2–C3R–C4R 179.3(5)°, C2–C3R–C4R–C5R 174.1(6)°. This is smaller than the twist observed in the benzothiophene derivative **28** where they are 161.8(5)/−178.8(5)/171.3(6)° (Table 2). This small out-of-plane twist may be a consequence of crystal packing but rotation of the ligand about the μ-C–vinyl bond is not expected to diminish electronic communication with the metal cluster [5]. The pyrrolidine donor, however, does lie almost co-planar with the thiophene [torsion angles C5R–C6R–C7R–N31 = 178.9(6)°; N31–C7R–S1–C4R = −178.7(5)°] and this reflects the high degree of positive charge, which must be resident on the nitrogen atom.

The μ(CO) moiety has typical distances with the Fe–C bond lengths of 1.902(7) and 1.915(6) Å and with both CO bond lengths 1.181(6) Å. The Fe–C_O–Fe bond angle is 83.5(2)° in contrast to the 81.8(3)° for the bridging μ-CCH_3 in Fe–C_C–Fe. The Fe–$CO_{bridging}$ angles are 138.2(5)/139.9(5)° and the Fe–C–CH_3 angles are 137.8(4)/138.6(4)°, with little difference between the two sets of angles. The terminal carbonyl ligands are eclipsed with respect to one another with 1.7(2)° for

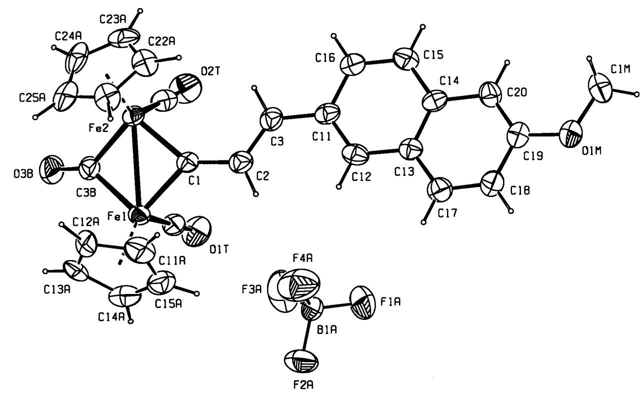

Fig. 4. ORTEP diagram of the major conformation of the iron dimer cation and tetrafluoroborate anion in **15**. Displacement ellipsoids are depicted at the 30% level.

O1T···Fe1–Fe2···O2T. The intermolecular interactions are primarily C–H···F and C–H···O in nature of which C6R–H6R···F(4A)^i, C···F 3.380(17) Å, C–H···F^i 172° and C16A–H16A···O3B, C···O 3.341(16) Å, C–H···O^{ii} 135° are representative and will not be discussed further. A representative ORTEP view of the cationic species in **15** is depicted as Fig. 4, and selected bond lengths and angles are listed in Table 2.

The Fe–$CO_{terminal}$ bond lengths are normal, 1.748(7), 1.757(9) Å and the Fe–CO angles are close to linearity (as expected) 179.3(6)/176.4(7)°; the two terminal CO distances are 1.137(8) and 1.139(9) Å. The bridging μ(C–CH) ligand $Fe_{1,2}$–C distances are 1.847(6) and 1.843(6) Å, with a C1–C2 bond length of 1.400(9), C2–C3R 1.330(10), C3–C11 1.453(9) Å indicating that the C1–C2/C3–C11 distances do not deviate much from normal sp^2–sp^2 bond lengths [1.46 Å] (c.f. **9** described above): the C=C bond length of 1.330(10) Å is similar to a normal Csp^2=sp^2 bond, [however, caution must be invoked when making comparisons as the e.s.d.'s of these CC bond lengths are rather large]. The μ(CO) moiety exhibits typical distances with the Fe–C bond lengths of 1.924(7) and 1.941(7) Å and a CO bond length of 1.162(8) Å. The Fe–C_O–Fe bond angle at CO is 81.0(3)° compared with the 85.8(3)° for Fe–C_C–Fe at the bridging μ-CCHCHR ligand. The Fe–C–O_μ angles are 140.1(6)/138.9(6)° and the Fe–C–CH_3 angles are 140.1(5)/134.1(5)°, perhaps indicating some asymmetry. The terminal carbonyl ligands are eclipsed with respect to one another with a dihedral angle of 1.6(2)° for O1T···Fe1–Fe2···O2T. The ligand lies in a slightly twisted arrangement with respect to the plane defined by the two iron atoms and the μ-carbon [with dihedral angles Fe1–C1–C2–C3 10.4(11)°, C1–C2–C3–C11, 175.1(6)° and C2–C3–C11–C12, 9.3(11)°]. This is not as large as the twist observed in the benzothiophene derivative, **29**, 161.8(5)/−178.8(5)/171.3(6)°. There are no classical hydrogen bonds in the crystal structure although there are some C–H···F contacts which will not be discussed, as they are rather weak and involve disordered $[BF_4]^-$ residues.

In **15** the O1M–C19–C18 and O1M–C19–C20 angles are markedly different at 114.4(7) and 125.5(7)°. This asymmetry is a structural feature of arylethers with the Cambridge Structural Database giving angles of 115.5 and 124.7° [33,34] and has been the subject of much discussion in the literature [32,33]. It has been suggested that conjugation of a lone pair on the O atom with the aromatic π system causes the methoxy group to lie in the plane of the aryl group: whilst steric interactions between the methyl CH_3 and the phenyl/naphthyl-H atoms may be responsible for the asymmetry in the reported O–C–C angles.

In Table 2 we have compared bond lengths and angles of **1** with those of **9**, **15** and some related compounds. It can be seen that the Fe–Fe and bridging Fe–C_O 1.95 Å bond lengths (mean) are comparable. However, the bridging Fe–C_C bond lengths (1.84 Å mean) are ca. 0.05–0.10 Å shorter than those in **9**, **27** and **29** and similar to those in **15** and the benzothiophene salt **28** reported by us previously [8b]. Although it may not be valid to compare **1** with the other compounds in Table 2, due to large vibrational motion in the molecular structures of the two independent Fe_2 cationic systems in **1**, it is valid to compare these others amongst themselves. It can be seen that the strong donor end groups cause an increase in the Fe–C_C distances but a decrease in the C_C–C (C_μ–C) as the ground state structure tends towards the cyanine limit. It implies that with the more positively charged C_μ atoms, there is more donation of electrons from the iron atoms into the unhybridised P_z orbital on C_μ and greater Fe–C_μ bond order. In **30** these Fe–C_C distances are even greater, perhaps due to the tetrahedral nature of C_μ.

2.5. NLO properties of 6a, 6b, 7a, 7b, 18, 19, 21, 22 and 26

The efficiency of SHG for **6a**, **6b**, **7a**, **7b**, **18**, **19**, **21**, **22** and **26** was assessed using the Kurtz powder method [10]. The samples were prepared by slow diffusion of diethyl ether into a CH_2Cl_2 solution of the salts in order to form microcrystalline powders that were then mulled to a fine powder and compacted in the sample holder. Grain sizes were not standardised. All the measurements were performed at the Nd:YAG laser fundamental wavelength (1064 nm). Other details of our experimental setup have been reported elsewhere [1f]. Unsurprisingly the values for the shorter chromophores **6a** (achiral), **6b** (chiral), **18** (*R*/*S* and racemate) **21** (*R*/*S* and racemate) and **22** (*R*/*S* and racemate) which exhibit UV absorbances around the second harmonic at 532, were all 0 times the urea standard. Unfortunately the longer chromophores **7a** (achiral), **7b** (chiral), **19** (*R*/*S* and racemate) and **26** (enriched *R*/*S* and racemate), which do not absorb at the second harmonic, also gave values ca. 0 times the urea standard.

It is important to stress that results obtained with the Kurtz powder technique [10] are very difficult to interpret in terms of molecular structure–property relationships, since they depend not only on the molecular hyperpolarisability β, but also very strongly on the crystal packing structure, grain size and phase-matching properties etc. Efficiencies as high as 100 times urea have been recorded for a perfectly aligned chiral ferrocene derivative of nitrobenzene but closely related compounds gave rise to much lower values ranging from 0 to 20 times urea despite their comparable molecular hyperpolarisabilities [12b,12c]. Even higher SHG has been observed by Marder and co-workers for a pyridinium derivative of ferrocene (220 times urea) [13] but was measured at just over one-third of this value by Daran and Manoury more recently [35]. Indeed many recorded attempts to produce chiral organometallic [36] or organic [37] NLO chromophores result in 0 or negligible powder efficiencies and these results have often been explained in terms of unfavourable alignment of otherwise highly NLO chromophores in the crystal lattice. Often the molecular hyperpolarisabilities are unreported for these compounds. The situation is further complicated by the general unpredictability of crystal packing from the molecular structure. Minute changes in peripheral groups or even crystallisation conditions can have a drastic effect on packing and ultimately the NLO properties. Unfortunately, we were unable to grow crystals of the chiral chromophores in either series in order to assess the packing in our compounds by examination of the angle between the molecular CT axis and the polar crystal axis if one is present.

Although zero bulk responses were obtained in our study, it does not follow that the molecular hyperpolarisabilties of these compounds are intrinsically zero. Previously we have recorded some extremely high β-values for organometallic merocyanines which incorporate the powerfully accepting $[(C_5H_5)_2Fe_2(CO)_2(\mu\text{-}CO)(\mu\text{-}C\text{–})]^+$ $[BF_4]^-$ residue [8]. The HRS technique [7] was used to obtain the hyperpolarisability (β) of our most promising compounds **6** and **7** at 1064 nm using the external reference method. No fluorescence was detected at 532 nm, the second harmonic frequency, in any of the cases but for compounds **6** the principle absorption band falls at this frequency and so, as expected, no second harmonic light was observed due to absorption. For compounds **7** however, β-values were obtained. In the achiral **7a**, $\beta = 826 \times 10^{-30}$ esu and for chiral **7b**, $\beta = 964 \times 10^{-30}$ esu. Generally β-values for organometallic chromophores fall within 50–700×10^{-30} esu [2] and comparison of our results with this range demonstrate that chomophores **7**, and probably **6**, represent extremely efficient NLO molecules. It is noteworthy that **7b** which incorporates the more highly strained nitrogen-donor ring affords the higher β-value.

3. Conclusions

The first examples of chiral D-π-A derivatives of **1** have been prepared. This was achieved by the inclusion of a chiral donor ((*S*)-(−)-2-methoxymethylpyrrolidine) to afford **6b** and **7b** or the use of the chiral bridging 1,1′-binaphthyl element to afford **18**, **19**, **21**, **22** and **26** (in both the racemic and *R* and *S* series). X-ray structural analysis of the paradigm complex **1** is reported for the first time along with structures for **9** and **15**, representative of the two classes of chromophores. Unfortunately measurement of the solid state NLO properties by the Kurtz powder technique [10] afforded zero SHG bulk efficiencies which may be explained in terms of unfavourable alignment of the dipoles in the crystal lattice. Measurement of compounds **6** and **7** by the HRS technique revealed that this series exhibits very high molecular hyperpolarisabilities (up to 964×10^{-30} esu). Work is ongoing to design and synthesise the next generation of chromophores derived from **1** that will exhibit both high molecular and bulk SHG.

4. Experimental

4.1. General methods

All reactions were performed under a nitrogen atmosphere. Tetrahydrofuran was freshly distilled from sodium benzophenone ketyl. $[Fe_2(\eta^5\text{-}C_5H_5)_2(CO)_2(\mu\text{-}CO)(\mu\text{-}C\text{-}CH_3)]^+ [BF_4]^-$, **1**, was prepared according to the literature procedure [3]. All other chemicals and reagents were used as received without further purification. Melting points were recorded on an Electrothermal digital melting point apparatus and are uncorrected. ^{1}H-NMR spectra were obtained on a Varian INOVA-300 MHz spectrometer or a Varian INOVA-500 MHz spectrometer. ^{13}C-NMR spectra were obtained on a Varian INOVA-300 MHz spectrometer or a Varian INOVA-500 MHz spectrometer operating at 75 and 126 MHz, respectively. FT-IR spectra were obtained on a Perkin–Elmer Paragon 1000 as either a solution in CH_2Cl_2 (windows: KBr, path length 0.1 mm) or in a KBr pellet (relative peak heights are given in parenthesis). UV–vis spectra were obtained on a UnicamUV2 spectrometer. Optical rotations were performed on a Perkin–Elmer 241 polarimeter at 546 nm, in CH_2Cl_2 at $c = 0.1$ g/100 ml in a cell of path length 10 cm. Spectroscopic assignments and analytical data are given for the racemic compounds; where appropriate the data for the enantiopure compounds are in agreement with these findings. The efficiency of SHG was measured using the Kurtz powder method [10]. Our experimental setup is described elsewhere [1f]. The filtered second harmonic signals emitted by a randomly sized sample placed in the holder were collected at a photomultiplier and measured with a 2 GS/s digital oscilloscope, which automatically integrates the signal. This integral is proportional to the SHG efficiency and a quantitative value was extracted by comparing it with its correspondent from a reference material (urea or KDP) obtained under the same experimental conditions.

4.2. (*S*)-(−)-5-(2-Methoxymethyl-pyrrolidin-1-yl)-thiophene-2-carbaldehyde (**2b**)

Following the procedure of Prim et al. [17] (*S*)-(+)-2-(methoxymethyl)-pyrrolidine (0.345 g, 3.0 mmol) and 5-bromothiophene-2-carboxaldehyde (0.570 g, 3.0 mmol) were added to water (10 ml) and heated at reflux for 12 h. The cooled mixture was extracted with Et_2O (2×50 ml) and the combined organic extracts were dried over $MgSO_4$. The solvent was removed in vacuo and the residue was purified by column chromatography on silica gel with 30:70 Et_2O–CH_2Cl_2 as the eluant to afford the title compound as a light brown oil (0.34 g) in 50% yield. $[\alpha]^{Hg}_{546}$ −178°. ^{1}H-NMR (300 MHz, $CDCl_3$): δ 9.49 (s, 1H, C*H*O), 7.47 (d, 1H, $J = 4.4$ Hz, Th), 5.97 (d, 1H, $J = 4.4$ Hz, Th), 3.86 (m, 1H, NC*H* (CH_2OMe)CH_2), 3.24–3.53 (m, 4H, CH_2NCH(CH_2OMe)CH_2), 3.36 (s, 3H, OMe), 2.11 (m, 4H, CH_2C$H_2$$CH_2$NCH). ^{13}C-NMR (75 MHz, $CDCl_3$): δC 180.2, 164.6, 140.4, 126.5, 103.8, 72.2, 62.4, 59.5, 29.4, 24.2. IR (CH_2Cl_2, cm^{-1}): 1633.9 (10, ν_{CO}), 1534.6 (4), 1371.8 (2), 1351.8 (1), 1141.4 (1), 1110.4 (2), 1055.8 (5). IR (KBr, cm^{-1}): 1635.6 (9, ν_{CO}), 1534.5 (5), 1490.8 (10), 1397.5 (1), 1370.3 (2), 1350.7 (1), 1264.8 (2), 1249.2 (2), 1139.9 (1), 1109.5 (2), 1054.4 (4), 976.0 (1), 922.1 (1), 744.2 (1), 660.0 (1). UV–vis (CH_2Cl_2): λ_{max} 368 nm; UV–vis (MeCN): λ_{max} 367 nm. Anal. Calc. for $C_{11}H_{15}NO_2S$: C, 58.67; H, 6.67; N, 6.22. Found: C, 58.84; H, 6.58; N, 5.98%.

4.3. Preparation of (*Z*)-(*E*)-3-(5-piperidin-1-yl-thiophen-2-yl)-propenal (**3a**)

5-Piperidin-1-yl-thiophene-2-carboxaldehyde (0.230 g, 1.20 mmol) and 2-tributylphosphinoacetaldehyde diethyl acetal bromide (2.00 g, 5.0 mmol) were dissolved in dry THF (25 ml) and potassium *tert*-butoxide (1.00 g, 8.9 mmol) was added. The reaction was stirred at room temperature (r.t.) overnight. The mixture was then filtered through a plug of alumina in a Hirsch funnel followed by washing with Et_2O (2×50 ml). The solution was evaporated to dryness and dissolved in THF (50 ml). Oxalic acid dihydrate (1.5 g, 11.9 mmol) was dissolved in water (20 ml) and added to the reaction mixture. There was an immediate colour change to dark green and the solution was stirred for a further 1 h. The mixture was extracted with Et_2O (1 × 100 ml) and the aq. layer was neutralised with K_2CO_3 before being extracted again with Et_2O (2 × 100 ml). The combined extracts were washed with K_2CO_3 (10% solution in water) and water (2 × 100 ml) and dried over $MgSO_4$ before being evaporated to dryness. Recrystalisation from C_6H_{14} afforded the title compound as a yellow crystalline solid (0.252 g) in 95% yield. M.p. 91.0–93.5 °C. ^{1}H-NMR (270 MHz, $CDCl_3$): δ 9.44 (d, 1H, $J = 7.9$ Hz, C*H*O), 7.41 (d, 1H, $J = 15.0$ Hz, ThC*H*=CHCHO), 7.10 (d, 1H, $J = 4.4$ Hz, Th), 6.08 (dd, 1H, $J = 7.9$, 15.0 Hz, ThCH=C*H*CHO), 6.00 (d, 1H, $J = 4.2$ Hz, Th), 3.29 (t, 4H, $J = 5.13$ Hz, C*H*$_2$NC*H*$_2$), 1.65 (m, 6H, piperidine). ^{13}C-NMR (75 MHz, $CDCl_3$): δ 192.6, 165.0, 146.2, 136.5, 123.4, 121.0, 104.5, 51.4, 25.2, 23.8. IR (CH_2Cl_2, cm^{-1}): 1657 (6, ν_{CO}), 1600 (10), 1526 (3), 1480 (9), 1383 (1), 1367 (1), 1124 (8), 1067 (5). IR (KBr, cm^{-1}): 1651 (10, ν_{CO}), 1597 (10), 1564 (4), 1525 (5), 1479 (9), 1445 (8), 1386 (3), 1367 (3), 1314 (3), 1240 (5), 1133 (5), 1118 (9), 1068 (7), 1041 (2), 1014 (2), 950 (3), 890 (2), 858 (2), 818 (2), 749 (3), 612 (2), 565 (2), 522 (1). UV–vis (CH_2Cl_2): λ_{max} 424 nm; UV–vis (MeCN): λ_{max} 418 nm. Anal. Calc. for $C_{12}H_{15}NOS$: C, 65.12; H, 6.83; N, 6.33. Found: C, 64.90; H, 6.81; N, 6.30%.

4.4. (*S*)-(−)-(*E*)-3-[5-(2-Methoxymethyl-pyrrolidin-1-yl)-thiophen-2-yl]-propenal (**3b**)

Following the procedure above **2b** (0.200 g, 0.89 mmol), 2-tributylphosphinoacetaldehyde diethyl acetal bromide (1.40 g, 3.50 mmol) and potassium *tert*-butoxide (1.00 g, 8.9 mmol) were dissolved in dry THF (25 ml) and stirred overnight under nitrogen. Work-up as above and purification by column chromatography on silica gel with 30:70 Et_2O–CH_2Cl_2 as the eluant afforded the title compound as a light brown oil (0.203 g) in 91% yield. $[\alpha]_{546}^{Hg}$ −155°. ^{1}H-NMR (300 MHz, $CDCl_3$): δ 9.44 (d, 1H, $J = 8.1$ Hz, C*H*O), 7.40 (d, 1H, $J = 14.9$ Hz, ThC*H*=CHCHO), 7.10 (d, 1H, $J = 4.2$ Hz, Th), 6.07 (dd, 1H, $J = 7.9$, 14.9 Hz, ThCH=C*H*CHO), 5.89 (d, 1H, $J = 4.2$ Hz, Th), 3.82 (m, 1H, NC*H*(CH_2OMe)CH_2), 3.13–3.60 (m, 4H, C*H*$_2$NCH(C*H*$_2$OMe)CH_2), 3.49 (s, 3H, OMe), 2.02–2.19 (m, 4H, C*H*$_2$C*H*$_2$$CH_2$NCH). ^{13}C-NMR (75 MHz, $CDCl_3$): δ 192.5, 161.0, 146.2, 136.8, 122.7, 120.3, 103.6, 72.6, 62.5, 59.5, 52.0, 29.4, 24.2. IR (CH_2Cl_2, cm^{-1}): 1655.1 (7, ν_{CO}), 1600.9 (9), 1526.0 (5), 1385.2 (1), 1354.1 (2), 1197.4 (1), 1124.5 (10), 1054.7 (4). IR (KBr, cm^{-1}): 1656 (5, ν_{CO}), 1599 (5), 1526 (6), 1455 (10), 1386 (1), 1353 (2), 1195 (1), 1124 (7), 1054 (3), 1000 (1), 948 (1), 817 (1), 753 (1). UV–vis (CH_2Cl_2): λ_{max} 429 nm; UV–vis (MeCN): λ_{max} 425 nm. Anal. Calc. for $C_{13}H_{17}NO_2S$: C, 62.12; H, 6.82; N, 5.57. Found: C, 61.51; H, 6.71; N, 5.42%.

4.5. Preparation of (*E*)-1-[5-(2-thiophen-2-yl-vinyl)-thiophen-2-yl]-piperidine (**4**)

5-Piperidin-1-yl-thiophene-2-carboxaldehyde (0.390 g, 2.0 mmol) and diethyl(2-thienylmethyl)phosphonate [18] (1.0 g, 4.30 mmol) were dissolved in dry THF (25 ml) and potassium *tert*-butoxide (0.495 g, 4.5 mmol) was added. The reaction was stirred overnight and quenched with water (50 ml). The mixture was extracted with Et_2O (50 ml), washed with water (2 × 50 ml) and dried over $MgSO_4$ followed by removal of the solvent. The residue was purified by column chromatography on silica gel with 1:1 CH_2Cl_2–petroleum ether as the eluant to afford the title compound in 84% yield (0.462 g), as a mixture of isomers in the *Z*–*E* ratio 1:3 (by NMR). Crystallisation from C_6H_{14} afforded the major isomer as yellow crystals: m.p. 126.5–127.5 °C. ^{1}H-NMR (300 MHz, $CDCl_3$): δ 7.08 (d, 1H, $J = 4.8$ Hz, Th), 6.94 (m, 2H, Th), 6.90 (d, 1H, $J = 16.0$ Hz, ThC*H*=CHTh), 6.71 (d, 1H, $J = 3.3$ Hz, Th), 6.68 (d, 1H, $J = 16.0$ Hz, ThCH=C*H*Th), 5.91 (1H, d, $J = 3.95$ Hz, Th), 3.17 (t, 4H, $J = 5.27$ Hz, C*H*$_2$NC*H*$_2$), 1.71 (m, 4H, piperidine), 1.57 (m, 2H, piperidine). ^{13}C-NMR (75 MHz, $CDCl_3$): δ 159.3, 143.7, 128.3, 127.7, 127.2, 124.5, 123.1, 123.0, 116.9, 104.3, 52.2, 25.4, 24.0. IR (CH_2Cl_2, cm^{-1}): 1610 (1), 1541 (2), 1514 (5), 1482 (10), 1385 (2), 1227 (2), 1190 (0.5), 1182 (0.5), 1130 (1), 1061 (1), 1012 (1), 936 (2). IR (KBr, cm^{-1}): 1577 (10), 1542 (1), 1541 (4), 1483 (6), 1446 (7), 1426 (5), 1384 (3), 1247 (4), 1226 (3), 1190 (1), 1181 (1), 1126 (2), 1062 (2), 1012 (2), 936 (3), 888 (2), 861 (1), 833 (2), 756 (2), 699 (3). UV–vis (CH_2Cl_2): λ_{max} 395 nm; UV–vis (MeCN): λ_{max} 390 nm; UV–vis (C_6H_{14}): λ_{max} 383 nm. Anal. Calc. for $C_{15}H_{17}NS_2$: C, 65.41; H, 6.22; N, 5.09. Found: C, 65.05; H, 5.89; N, 5.03%.

4.6. (*E*)-5-[2-(5-Piperidin-1-yl-thiophen-2-yl)-vinyl]-thiophene-2-carbaldehyde (**5**)

Compound **4** (0.275 g, 1.0 mmol) was dissolved in dry THF (15 ml) and cooled to −78 °C. BuLi (1.6 ml, 4.0 mmol, 2.5 mol. sol. in C_6H_{14}) was added dropwise and the mixture was stirred for 1 h. DMF (0.5 ml, 6.4 mmol) was introduced and the reaction was allowed to warm to r.t. The mixture was diluted with Et_2O (50 ml) and quenched with water (100 ml). Extraction with Et_2O (50 ml), washing with water (4 × 50 ml), drying over $MgSO_4$ followed by removal of the solvent afforded a red solid. Purification by column chromatography on silica gel with CH_2Cl_2 as the eluant afforded the title compound in 96% yield (0.29 g). Recrystallisation from Et_2O–C_6H_{14} gave red plates: m.p. 139.5–141.0 °C. ^{1}H-NMR (300 MHz, $CDCl_3$): δ 9.78 (s, 1H, C*H*O), 7.59 (d, 1H, $J = 4.0$ Hz, Th), 7.14 (d, 1H, $J = 15.6$ Hz, ThC*H*=CHTh), 6.97 (d, 1H, $J = 4.0$ Hz, Th), 6.85 (d, 1H, $J = 4.2$ Hz, Th), 6.60 (d, 1H, $J = 15.6$ Hz, ThCH=C*H*Th), 5.93 (d, 1H, $J = 4.0$ Hz, Th), 3.22 (t, 4H, $J = 5.05$ Hz,

CH_2NCH_2), 1.71 (m, 4H, piperidine), 1.57 (m, 2H, piperidine). ^{13}C-NMR (75 MHz, $CDCl_3$): δ 182.4, 161.2, 154.3, 140.1, 137.9, 130.6, 127.6, 126.6, 124.8, 114.8, 104.2, 51.9, 25.4, 24.0. IR (CH_2Cl_2, cm^{-1}): 1656 (10, ν_{CO}), 1600 (6), 1538 (2), 1515 (5), 1489 (5), 1383 (4), 1229 (10), 1130 (1), 1063 (3), 1048 (5), 1021 (1), 1013 (1), 936 (2). IR (KBr, cm^{-1}): 1643 (7, ν_{CO}), 1589 (6), 1582 (3), 1516 (5), 1432 (10), 1370 (3), 1352 (2), 1288 (3), 1264 (2), 1229 (5), 1122 (1), 1068 (2), 1045 (4), 1007 (2), 934 (4), 892 (2), 857 (2), 828 (3), 800 (2), 756 (4), 738 (1), 650 (2), 530 (2). UV–vis (CH_2Cl_2): λ_{max} 470 nm; UV–vis (MeCN): λ_{max} 462 nm; UV–vis (C_6H_{14}): λ_{max} 443 nm. Anal. Calc. for $C_{16}H_{17}NOS_2$: C, 63.33; H, 5.65; N, 4.62. Found: C, 63.39; H, 5.65; N, 4.53%.

4.7. General procedure for the condensation of $[Fe_2(\eta^5\text{-}C_5H_5)_2(CO)_2(\mu\text{-}CO)(\mu\text{-}C\text{–}CH_3)]^+$ $[BF_4]^-$ (**1**) with aldehydes

Following the procedure of Casey et al. [4], **1** (one equivalent) and the required aldehyde (two equivalents) were stirred at reflux in CH_2Cl_2 (5–10 ml). The reactions were monitored by IR spectroscopy for the disappearance of the ν_{CO} bands of the starting material that took ca. 18 h. The volume of the solvent was reduced in vacuo to half the original amount and the product was isolated by precipitation by the addition of Et_2O (50–100 ml). The precipitate was collected by filtration and redissolved in a minimum volume of CH_2Cl_2 before being reprecipitated by the addition of Et_2O (100 ml). This was repeated and the solid was dried under high vacuum.

4.7.1. $[Fe_2(\eta^5\text{-}C_5H_5)_2(CO)_2(\mu\text{-}CO)(\mu\text{-}(E)\text{-}C\text{–}CH{=}CH\text{-}2\text{-}(5\text{-piperidin-1-yl-thiophene}))]^+$ $[BF_4]^-$ (**6a**)

Experimental procedures and work-up were as described above. Experimental details: 5-piperidin-1-yl-thiophene-2-carboxaldehyde (0.250 g, 1.28 mmol), **1** (0.220 g, 0.50 mmol). Obtained as a dark red solid. Yield: 0.170 g, 55% based on **1**. ^{1}H-NMR (500 MHz, CD_2Cl_2): δ 8.61 (d, 1H, $J = 12.2$ Hz, ThCH=C*H*-μC), 8.20 (d, 1H, $J = 4.9$ Hz, Th), 7.74 (d, 1H, $J = 12.2$ Hz, ThC*H*=CH-μC), 6.77 (d, 1H, $J = 4.6$ Hz, Th), 5.06 (10H, s, Cp), 3.79 (bs, 4H, CH_2NCH_2), 1.60–1.90 (bm, 6H, piperidine). ^{13}C-NMR (75 MHz, CD_2Cl_2): δC 349.4 (μ-*C*), 262.0 (μ-*C*O), 209 (^{t}*C*O), 176.7, 152.8, 145.0, 143.7, 125.7, 115.8, 89.8, 50.7, 26.3, 23.3. IR (CH_2Cl_2, cm^{-1}): 2013 (10, CO), 1982 (2, CO), 1820 (4, CO), 1515 (6), 1456 (6), 1160 (5), 1137 (1), 1100 (3), 1060 (3). IR (KBr, cm^{-1}): 1996 (10, CO), 1966 (4, CO), 1805 (5), 1522 (6), 1442 (10), 1245 (6), 1170 (9), 1084 (4), 888 (1), 852 (1), 779 (1), 707 (1), 616 (2), 551 (1), 497 (2). UV–vis (CH_2Cl_2): λ_{max} (ε) 557 nm (79 560 M^{-1} cm^{-1}); UV–vis (MeCN): λ_{max} (ε) 547 nm (67 770 M^{-1} cm^{-1}). Anal. Calc. for $C_{25}H_{24}BF_4Fe_2NO_3S\cdot 0.4CH_2Cl_2$: C, 64.82; H, 3.81; N, 2.15. Found: C, 46.75; H, 3.79; N, 1.93%.

4.7.2. (*S*)-$[Fe_2(\eta^5\text{-}C_5H_5)_2(CO)_2(\mu\text{-}CO)(\mu\text{-}(E)\text{-}C\text{–}CH{=}CH\text{-}2\text{-}(5\text{-}(2\text{-methoxymethyl-pyrrolidin-1-yl})\text{-thiophene}))]^+$ $[BF_4]^-$ (**6b**)

Experimental procedures and work-up were as described above. Experimental details: **2b** (0.100 g, 0.44 mmol), **1** (0.100 g, 0.23 mmol). Obtained as a dark red solid. Yield: 0.077 g, 52% based on **1**. ^{1}H-NMR (500 MHz, CD_2Cl_2): δ 8.73 (d, 1H, $J = 12.2$ Hz, ThCH=C*H*-μC), 8.09 (bs, 1H, Th), 7.82 (d, 1H, $J = 12.02$ Hz, ThC*H*=CH-μC), 6.69 (bs, 1H, Th), 5.06 (s, 10H, Cp), 4.34 (bs, 1H, NC*H*(CH_2OMe)CH_2), 3.50–3.90 (bm, 4H, CH_2NCH(CH_2OMe)CH_2), 3.37 (s, 3H, O*Me*), 2.20–2.30 (bm, 4H, $CH_2CH_2CH_2$NCH). ^{13}C-NMR (75 MHz, CD_2Cl_2): δC 350.3 (μ-*C*), 262.9 (μ-*C*O), 209.0 (^{t}*C*O), 174.2, 152.0, 145.5, 143.7, 126.6, 117.0, 72.6, 64.7, 59.7, 54.0, 29.3, 24.1. IR (CH_2Cl_2, cm^{-1}): 2014 (10, CO), 1981 (2, CO), 1821 (4, CO), 1605 (3), 1507 (7), 1375 (2), 1218 (2), 1190 (2), 1170 (8), 1113 (3), 1061 (3). IR (KBr, cm^{-1}): 1998 (9, CO), 1965 (4, CO), 1803 (4, CO), 1572 (1), 1510 (6), 1439 (10), 1374 (3), 1282 (2), 1246 (4), 1219 (5), 1169 (9), 1104 (4), 1084 (5), 914 (1), 851 (1), 778 (1), 708 (1), 629 (2), 587 (3), 551 (2). UV–vis (CH_2Cl_2): λ_{max} (ε) 556 nm (56 960 M^{-1} cm^{-1}); UV–vis (MeCN): λ_{max} (ε) 547 nm (51 830 M^{-1} cm^{-1}). Anal. Calc. for $C_{26}H_{26}BF_4Fe_2NO_4S\cdot 0.8CH_2Cl_2$: C, 44.97; H, 3.86; N, 1.96. Found: C, 44.95; H, 3.86; N, 1.46%.

4.7.3. $[Fe_2(\eta^5\text{-}C_5H_5)_2(CO)_2(\mu\text{-}CO)(\mu\text{-}(E)\text{-}C\text{–}CH{=}CH\text{–}CH{=}CH\text{-}2\text{-}(5\text{-piperidin-1-yl-thiophene}))]^+$ $[BF_4]^-$ (**7a**)

Experimental procedures and work-up were as described above. Experimental details: **3a** (0.090 g, 0.41 mmol), **1** (0.090 g, 0.20 mmol). Obtained as a dark blue solid. Yield: 0.084 g, 67% based on **1**. ^{1}H-NMR (500 MHz, CD_2Cl_2): δ 8.67 (d, 1H, $J = 10.0$ Hz, ThCH=CH–CH=C*H*–μC), 7.85 (d, 1H, $J = 11.2$ Hz, ThC*H*=CH–CH=CH–μC), 7.76 (bs, 1H, Th), 7.47 (dd, 1H, $J = 2 \times 10.3$ Hz, ThCH=C*H*–CH=CH–μC), 6.72 (bs, 1H, Th), 6.42 (dd, 1H, $J = 2 \times 10.3$ Hz, ThCH=CH–C*H*=CH–μC), 5.02 (s, 10H, Cp), 4.87 (bs, 4H, CH_2NCH_2), 1.60–1.95 (bm, 6H, piperidine). ^{13}C-NMR (75 MHz, CD_2Cl_2): δC 339.8 (μ-*C*), 263.6 (μ-*C*O), 209.8 (^{t}*C*O), 175.8, 154.5, 149.8, 148.4, 147.7, 130.8, 118.9, 115.4, 89.4, 54.3, 26.2, 23.5. IR (CH_2Cl_2, cm^{-1}): 2009 (7, CO), 1981 (2, CO), 1815 (4, CO), 1586 (1), 1545 (3), 1470 (5), 1385 (3), 1360 (2), 1208 (3), 1191 (2), 1146 (10), 1092 (5), 1086 (5), 1018 (2). IR (KBr, cm^{-1}): 1993 (7, CO), 1959 (3, CO), 1801 (4, CO), 1618 (2), 1549 (4), 1473 (6), 1434 (10), 1384 (4), 1279 (1), 1254 (2), 1152 (9), 1132 (9), 1084 (8), 1015 (4), 886 (1), 852 (1), 732 (2), 614 (2), 494 (2). UV–vis (CH_2Cl_2): λ_{max} (ε) 658 nm (86 480 M^{-1} cm^{-1}). UV–vis (MeCN): λ_{max} (ε) 643 nm (59 580 M^{-1} cm^{-1}). Anal. Calc. for $C_{26}H_{26}BF_4Fe_2NO_3S\cdot 0.75CH_2Cl_2$: C, 46.20; H, 3.95; N, 2.02. Found: C, 46.26; H, 3.93; N, 1.90%.

4.7.4. (*S*)-[$Fe_2(\eta^5$-$C_5H_5)_2(CO)_2(\mu$-$CO)(\mu$-(*E*)-C–CH=CH–CH=CH-2-(5-(2-methoxymethyl-pyrrolidin-1-yl)-thiophene))]$^+$ [BF_4]$^-$ (**7b**)

Experimental procedures and work-up were as described above. Experimental details: **3b** (0.100 g, 0.40 mmol), **1** (0.100 g, 0.23 mmol). Obtained as a dark red solid. Yield: 0.103 g, 65% based on **1**. ^{1}H-NMR (500 MHz, CD_2Cl_2): δ 8.68 (d, 1H, $J = 11.2$ Hz, ThCH=CH–CH=C*H*–μC), 7.88 (d, 1H, $J = 12.2$ Hz, ThC*H*=CH–CH=CH–μC), 7.72 (bs, 1H, Th), 7.50 (dd, 1H, $J = 2 \times 12.0$ Hz, ThCH=C*H*–CH=CH–μC), 6.98 (bs, 1H, Th), 6.47 (dd, 1H, $J = 2 \times 12.2$ Hz, ThCH=CH–C*H*=CH–μC), 5.03 (s, 10H, Cp), 4.29 (bs, 1H, NC*H*(CH_2O-Me)CH_2), 3.50–3.90 (bm, 4H, CH_2NCH(CH_2O-Me)CH_2), 3.36 (s, 3H, O*Me*), 2.15–2.30 (bm, 4H, CH_2C$H_2$$CH_2$NCH). ^{13}C-NMR (75 MHz, CD_2Cl_2): δC 340.7 (μ-*C*), 263.5 (μ-*C*O), 209.8 (^{t}*C*O), 173.7, 154.8, 148.7, 148.5, 147.7, 131.6, 119.0, 117.0, 89.4, 73.2, 64.9, 59.5, 54.5, 29.4, 24.2. IR (CH_2Cl_2, cm^{-1}): 2010 (7, CO), 1983 (3, CO), 1816 (4, CO), 1605 (2), 1588 (1), 1537 (4), 1382 (4), 1348 (4), 1168 (9), 1148 (10), 1108 (10), 1081 (6). IR (KBr, cm^{-1}): 1995 (6, CO), 1963 (3, CO), 1804 (4, CO), 1580 (3), 1538 (3), 1434 (10), 1348 (3), 1167 (7), 1147 (7), 1104 (7), 1084 (7), 988 (2), 914 (1), 850 (1), 733 (1), 613 (1). UV–vis (CH_2Cl_2): λ_{max} (ε) 655 nm (97 300 M^{-1} cm^{-1}); UV–vis (MeCN): λ_{max} (ε) 640 nm (72 500 M^{-1} cm^{-1}). Anal. Calc. for $C_{28}H_{28}BF_4Fe_2NO_4S \cdot 1.34CH_2Cl_2$: C, 44.76; H, 3.89; N, 1.78. Found: C, 44.67; H, 4.01; N, 1.65%.

4.7.5. [$Fe_2(\eta^5$-$C_5H_4CH_3)_2(CO)_2(\mu$-$CO)(\mu$-(*E*)-C–CH=CH-2-(5-piperidin-1-yl-thiophene))]$^+$ [BF_4]$^-$ (**9**)

Compound **8** (0.100 g, 0.26 mmol), 5-piperidin-1-yl-thiophene-2-carboxaldehyde (**2a**), (0.250 g, 1.28 mmol) and tetraflouroboric acid diethyl etherate (five drops) were mixed in CH_2Cl_2 (5 ml) and heated at reflux for 4 h. Work-up by precipitation as above afforded the title compound as a dark red solid (0.130 g) in 77%. Crystallisation by diffusion of Et_2O into a CH_2Cl_2 solution of the product produced X-ray quality crystals. ^{1}H-NMR (500 MHz, $CDCl_3$): δ 8.65 (d, 1H, $J = 12.3$ Hz, ThCH=C*H*–μC), 8.10 (d, 1H, $J = 5.3$ Hz, Th), 7.79 (d, 1H, $J = 12.3$ Hz, ThC*H*=CH–μC), 6.71 (d, 1H, $J = 5.3$ Hz, Th), 4.65 (bs, 2H, Cp–Hα), 4.53 (bs, 2H, Cp–Hβ), 3.87 (m, 4H, CH_2NCH_2), 2.18 (s, 6H, Cp–*Me*), 1.83 (bs, 6H, piperidine). ^{13}C-NMR (75 MHz, $CDCl_3$): δC 353.6 (μ-*C*), 264.4 (μ-*C*O), 209.5 (^{t}*C*O), 176.0, 152.8, 144.9, 142.6, 125.4, 115.2, 51.8, 26.1, 23.5, 13.3. IR (CH_2Cl_2, cm^{-1}): 2009 (7, CO), 1976 (2, CO), 1816 (4, CO), 1619 (1), 1514 (5), 1383 (1), 1171 (10), 1160 (4), 1137 (2), 1100 (3), 1090 (3), 1064 (3). IR (KBr, cm^{-1}): 1992 (8, CO), 1962 (3, CO), 1802 (4, CO), 1619 (3), 1518 (7), 1441 (10), 1267 (5), 1246 (7), 1169 (10), 1137 (3), 1126 (3), 1084 (5), 886 (2), 853 (1), 778 (1), 707 (1), 615 (1), 582 (1), 551 (1), 498 (1). UV–vis (CH_2Cl_2): λ_{max} (ε) 562 nm (59 440 M^{-1} cm^{-1}); UV–vis (MeCN): λ_{max} (ε) 551 nm (52 680 M^{-1} cm^{-1}). Anal. Calc. for $C_{27}H_{28}BF_4Fe_2NO_3S \cdot 0.75CH_2Cl_2$: C, 46.98; H, 4.16; N, 1.98. Found: C, 46.93; H, 4.21; N, 1.99%. Structure also established by X-ray analysis.

4.8. 2,2′-Dimethoxy-3-(2-(5-thiophenecarboxaldehyde))-1,1′-binaphthalene (**17**)

KO^{t}Bu (0.112 g, 1.0 mmol) was added to a solution of 2,2′-dimethoxy-3-carboxaldehyde-1,1′-binaphthalene (**16**) (0.130 g, 0.38 mmol) (from (*R*)-1,1′-bi-2-naphthol [α]$_D$: +101.6° from (*S*)-1,1′-bi-2-naphthol [α]$_D$: −100.4°) and diethyl(2-thienylmethyl)phosphonate (0.234 g, 1.0 mmol) in dry THF (25 ml). The mixture was stirred at r.t. under an inert atmosphere for 1 h. The solution was then poured into a separating funnel charged with water (50 ml) and extracted with CH_2Cl_2 (2 × 50 ml). The organic extracts were combined, washed with water (2 × 50 ml) and dried over $MgSO_4$. After removal of the solvent, the yellow oil was purified by column chromatography on silica gel with 1:1 CH_2Cl_2–petroleum ether as the eluant to afford 2,2′-dimethoxy-3-(*E*-(2-(2-thienyl)ethene)-1,1′-binaphthalene as a yellow solid (0.120 g, 0.28 mmol) in 74% yield. M.p. 216–218 °C. ^{1}H-NMR (300 MHz, $CDCl_3$): δ 8.15 (s, 1H, C4–*H*), 8.00 (d, 1H, $J = 9.0$ Hz, C4′–*H*), 7.87 (d, 2H, $J = 7.9$ Hz, aryl), 7.00–7.56 (m, 12H, aryl, alkenyl, thienyl), 3.79 (s, 3H, OCH_3), 3.42 (s, 3H, OCH_3). ^{13}C-NMR (75 MHz, $CDCl_3$): δ 155.2, 154.6, 149.9, 137.9, 134.3, 133.9, 131.2, 130.8, 130.0, 129.4, 128.3, 128.2, 127.9, 126.9, 126.4, 126.3, 126.1, 125.8, 125.5, 125.3, 124.8, 124.3, 123.9, 123.8, 119.4, 113.9, 61.3, 56.8. IR (CH_2Cl_2, cm^{-1}): 2940 (1.5), 2840 (1.5), 1623 (4), 1594 (4.5), 1510 (4.5), 1460 (4), 1445 (7), 1357 (4), 1334 (2), 1236 (10), 1149 (4.5), 1103 (3.5), 1080 (5), 1046 (3.5), 1006 (4), 960 (3). IR (KBr, cm^{-1}): 2933 (1.5), 2838 (1), 1622 (4), 1592 (5), 1510 (4), 1496 (3), 1473 (3), 1452 (4), 1431 (3.5), 1405 (4), 1357 (4), 1334 (3.5), 1273 (10), 1262 (5), 1240 (5), 1147 (3.5), 1104 (4), 1080 (7), 1043 (2.5), 1007 (5), 956 (4.5), 933 (1), 910 (1), 893 (1.5), 850 (1.5), 805 (5), 776 (1.5), 763 (4.5), 746 (4), 710 (5), 612 (1.5), 600 (0.5), 493 (1.5). UV λ_{max} (CH_2Cl_2): 339 nm. Anal. Calc. for $C_{28}H_{22}O_2S \cdot 0.1CH_2Cl_2$: C, 78.33; H, 5.16. Found: C, 78.36; H, 5.12%. From *R*-1,1′-binaphthyl [α]$_D$: +185.5°. From *S*-1,1′-binaphthyl [α]$_D$: −184.3°.

BuLi (0.2 ml, 0.5 mmol, 2.5 mol. solution in C_6H_{14}) was introduced to a cooled solution (−78 °C) of 2,2′-dimethoxy-3-(*E*-(2-(2-thienyl)ethene)-1,1′-binaphthalene (0.11 g, 0.26 mmol) in dry THF (25 ml). The mixture was allowed to warm slowly to 0 °C over 1 h and DMF (0.5 ml) was added. The solution was stirred for a further 30 min at r.t. and then quenched by the addition of dilute HCl (50 ml, 0.1 mol). The mixture was diluted with CH_2Cl_2 (50 ml) and washed with water (4 × 50 ml). After drying the organic portion over $MgSO_4$ the solvent was removed in vacuo and a brown oil was obtained. This was purified by column chromatography on silica gel with CH_2Cl_2 as the eluant to afford the title compound as a yellow solid (0.109 g, 0.24 mmol) in 92% yield. M.p. (*R*-isomer) 187–190 °C. ^{1}H-NMR (300 MHz, $CDCl_3$): δ 9.86 (s, 1H, C*H*O), 8.19 (s, 1H, C4–*H*), 8.02 (d, 1H, $J=9.1$ Hz, aryl) 7.90 (d, 1H, $J=3.8$ Hz, aryl), 7.87 (d, 1H, $J=3.8$ Hz, aryl), 7.67 (d, 1H, $J=3.8$ Hz, aryl), 7.65 (d, 1H, $J=19.9$ Hz, CH=C*H*), 7.47 (d, 1H, $J=9.1$ Hz, aryl) 7.18–7.42 (m, 7H, aryl, thienyl), 7.22 (d, 1H, $J=19.9$ Hz, CH=C*H*), 7.20 (m, 1H, aryl), 3.80 (s, 3H, OCH_3), 3.42 (s, 3H, OCH_3). ^{13}C-NMR (75 MHz, $CDCl_3$): δ 182.8 (*C*O), 155.2, 154.6, 153.4, 141.9, 137.4, 134.5, 134.2, 131.1, 130.2, 129.7, 129.3, 129.1, 128.5, 128.3, 127.2, 127.0, 127.0, 126.8, 126.1, 125.8, 125.6, 125.3, 124.0, 122.8, 119.1, 113.8, 61.4, 56.8. IR (CH_2Cl_2, cm^{-1}): 1660 (10), 1606 (6), 1510 (1), 1497 (1), 1386 (1), 1358 (2), 1149 (2), 1104 (1), 1080 (2), 1048 (2.5), 1021 (0.5), 1005 (1). IR (KBr, cm^{-1}): 2931 (1), 2834 (1), 1657 (10), 1620 (4), 1591 (4), 1508 (3), 1495 (2.5), 1456 (7), 1437 (6.5), 1408 (2), 1357 (4), 1332 (3), 1266 (7), 1247 (6), 1220 (7), 1146 (4.5), 1101 (3), 1077 (5), 1045 (5), 1019 (3), 1004 (4.5), 951 (2), 906 (1), 893 (1), 807 (5), 778 (2), 748 (5), 663 (1), 643 (1), 608 (1), 534 (1), 476 (1). UV λ_{max} (CH_2Cl_2): 239, 378 nm. Anal. Calc. for $C_{29}H_{22}O_3S\cdot 0.35H_2O$: C, 767.27; H, 4.97. Found: C, 76.20; H, 5.00%. From *R*-1,1′-binaphthyl [α]$_D$: +221.1°. From *S*-1,1′-binaphthyl [α]$_D$: −222.9°.

4.9. 2,2′-Dimethoxy-6,6′-bis(E-2-(2-thienyl)ethene)-1,1′-binaphthalene (24)

According to the procedure in Section 4.8, diethyl(2-thienylmethyl)phosphonate [18] (0.468 g, 2.0 mmol) was reacted with 2,2′-dimethoxy-6,6′-dicarboxaldehyde-1,1′-binaphthalene (0.200 g, 0.54 mmol) followed by purification in the same way to afford the title compound as a yellow solid (0.162 g, 0.31 mmol) in 57% yield. M.p. (*R* and *S* isomers) 246.5–248 °C. ^{1}H-NMR (300 MHz, $CDCl_3$): δ 7.95 (d, 2H, $J=9.0$ Hz, aryl), 7.84 (d, 2H, $J=7.0$ Hz, aryl), 7.44 (d, 2H, $J=9.0$ Hz, aryl), 7.31 (dd, 2H, $J=9.1$, 1.9 Hz, aryl), 7.23 (d, 2H, $J=16.0$ Hz, CH=C*H*–thienyl), 7.17 (bd, 2H, $J=4.8$ Hz, thienyl), 7.08 (d, 2H, $J=8.6$ Hz, aryl), 7.05 (d, 2H, $J=16.0$ Hz, C*H*=CH–thienyl), 7.05 (bd, 2H, $J=2.6$ Hz, thienyl), 6.99 (dd, 2H, $J=5.0$, 3.7 Hz, thienyl), 3.77 (s, 6H, OCH_3). ^{13}C-NMR (75 MHz, $CDCl_3$): δ 155.6, 143.5, 138.0, 133.9, 132.6, 129.9, 128.9, 127.9, 126.9, 126.1, 126.0, 124.4, 124.1, 121.5, 119.9, 114.8, 57.1. IR (CH_2Cl_2, cm^{-1}): 1605 (10), 1498 (0.5), 1481 (1), 1339 (1), 1166 (0.5), 1096 (1.5), 1064 (1.5), 1044 (1.5). IR (KBr, cm^{-1}): 2931 (1), 2834 (1), 1621 (1.5), 1589 (5), 1497 (3), 1474 (5), 1459 (4.5), 1438 (2), 1334 (3), 1256 (10), 1023 (2), 1164 (2), 1095 (5), 1063 (5), 1042 (5), 947 (6), 888 (1), 855 (1), 824 (3), 803 (4), 696 (6), 668 (1). UV λ_{max} (CH_2Cl_2): 346, 360 (sh) nm. Anal. Calc. for $C_{34}H_{26}O_2S_2$: C, 76.98; H, 4.90. Found: C, 77.10; H, 5.17%. From *R*-1,1′-binaphthyl[α]$_D$: −495.3°. From *S*-1,1′-binaphthyl[α]$_D$: +486.5°.

4.10. 2,2′-Dimethoxy-6,6′-bis(E-2-(2-(5-thiophenecarboxaldehyde))ethenyl)-1,1′-binaphthalene (25)

According to the procedure in Section 4.6, BuLi (0.25 ml, 0.64 mmol, 2.5 mol. solution in C_6H_{14}) was reacted with **24** (0.100 g, 0.19 mmol) followed addition of DMF (0.5 ml) and acidic aq. quench to afford the title compound as a yellow solid (0.082 g, 0.13 mmol) in 68% yield. M.p. (*R*-isomer) 258–260 °C; (*S*-isomer) 252–253 °C. ^{1}H-NMR (300 MHz, $CDCl_3$): δ 9.84 (s, 2H, C*H*O), 7.99 (d, 2H, $J=9.0$ Hz, aryl), 7.90 (s, 2H, aryl), 7.64 (d, 2H, $J=4.0$ Hz, thienyl), 7.47 (d, 2H, $J=9.0$ Hz), 7.42 (dd, 2H, $J=9.0$, 1.3 Hz, aryl), 7.29 (d, 2H, $J=16.3$ Hz, C*H*=CH–thienyl), 7.19 (d, 2H, $J=16.0$ Hz, CH=C*H*–thienyl), 7.12 (d, 2H, $J=4.1$ Hz, thienyl), 7.10 (d, 2H, $J=9.7$ Hz, aryl), 3.79 (s, 6H, OCH_3). ^{13}C-NMR (75 MHz, $CDCl_3$): δ 182.8, 156.0, 153.1, 141.6, 137.5, 134.4, 133.4, 131.5, 130.3, 129.4, 128.5, 126.6, 126.1, 123.9, 120.4, 119.7, 114.8, 57.0. IR (CH_2Cl_2, cm^{-1}): 2842 (1), 1662 (10), 1616 (1.5), 1590 (2), 1384 (0.5), 1353 (1), 1232 (5), 1178 (1), 1096 (1), 1064 (1), 1048 (3), 953 (2). IR (KBr, cm^{-1}): 2832 (1), 2792 (1), 1657 (10), 1604 (4), 1588 (4), 1519 (0.5), 1495 (1), 1482 (1), 1447 (8), 1436 (8), 1351 (1.5), 1268 (6), 1254 (6), 1226 (7), 1166 (3), 1095 (3), 1063 (4), 1045 (5), 950 (2), 872 (1), 813 (3), 790 (2.5), 733 (0.5), 678 (0.5), 654 (0.5), 498 (0.5). UV λ_{max} (CH_2Cl_2): 392 nm. Anal. Calc. for $C_{36}H_{26}O_4S_2\cdot 1CH_2Cl_2$: C, 72.98; H, 3.97. Found: C, 73.08; H, 4.79%. From *R*-1,1′-binaphthyl [α]$_D$: −650.2°. From *S*-1,1′-binaphthyl [α]$_D$: +569.1°.

4.10.1. [2-(CH=CH-μ-C–Fe_2(μ-CO)(η^5-C_5H_5)$_2$(CO)$_2$)naphthalene]$^+$ [BF_4]$^-$ (13)

According to the procedure in Section 4.7, **1** (0.500 g, 1.15 mmol) was condensed with **10** (0.360 g, 2.3 mmol) to afford **13** as a red solid (0.370 g, 0.66 mmol) in 57% yield. ^{1}H-NMR (500 MHz, acetone-d_6): δ 10.41 (d, 1H, $J=15.0$ Hz, μ-CC*H*=CH), 8.90 (s, 1H, aryl), 8.38 (d, 1H, $J=14.9$ Hz, μ-CCH=C*H*), 8.13 (d, 2H, $J=8.7$ Hz, aryl), 8.05 (d, 1H, $J=8.4$ Hz, aryl), 7.77 (dd, 1H, $J=8.4$, 7.0 Hz, aryl), 7.76 dd, 1H, $J=7.9$, 7.0 Hz, aryl), 5.73 (s, 10H, C_5H_5). ^{13}C-NMR (126 MHz, acetone-d_6): δ 441.0 (μ-*C*CH=CH), 254.8 (μ-CO), 209.0 (^{t}CO), 153.0, 152.8, 138.5, 136.8, 134.6, 133.1, 130.4, 129.1, 128.5, 125.9, 93.2 (C_5H_5). IR (CH_2Cl_2, cm^{-1}): 2035 (10), 2002 (2.0), 1845 (4.5), 1545 (9). IR (KBr, cm^{-1}): 2028 (10), 1989 (8), 1854 (7.5), 1543 (9). UV λ_{max} (ε/M^{-1} cm^{-1}) (CH_2Cl_2): 468 nm (27 400). UV λ_{max} (ε/M^{-1} cm^{-1}) (CH_3CN): 441 nm (26 000). Anal. Calc. for $C_{26}H_{19}BF_4Fe_2O_3\cdot H_2O$: C, 52.41; H, 3.52. Found: C, 52.55; H, 3.60%.

4.10.2. [2-Methoxy-3-(CH=CH-μ-C–Fe$_2$(μ-CO)(η^5-C$_5$H$_5$)$_2$(CO)$_2$) naphthalene]$^+$ [BF$_4$]$^-$ (**14**)

As detailed in the procedure in Section 4.7, **1** (0.350 g, 0.8 mmol) was condensed with **11** (0.300 g, 1.6 mmol) to afford **14** as a red solid (0.328 g, 0.54 mmol) in 68% yield. ^{1}H-NMR (500 MHz, CD$_2$Cl$_2$): δ 10.13 (d, 1H, J = 14.6 Hz, μ-CCH=CH), 8.82 (1H, s, aryl), 8.22 (d, 1H, J = 14.6 Hz, μ-CCH=CH), 8.08 (d, 1H, J = 8.3 Hz, aryl), 7.82 (s, 1H, aryl), 7.66 (dd, 1H, J = 7.8, 7.3 Hz, aryl), 7.48 (dd, 1H, J = 7.8, 7.3 Hz, aryl), 7.31 (s, 1H, aryl), 5.40 (s, 10H, C$_5$$H_5$), 4.16 (s, 3H, OCH$_3$). ^{13}C-NMR (126 MHz, CD$_2$Cl$_2$): δ 437.7 (μ-CCH=CH), 253.7 (μ-CO), 207.8 (^{t}CO), 157.9, 153.2, 149.9, 138.8, 135.3, 131.1, 130.7, 129.7, 127.6, 126.1, 124.7, 107.7, 92.4 (C_5H$_5$), 57.0 (OCH$_3$). IR (CH$_2$Cl$_2$, cm^{-1}): 2033 (10), 2004 (2), 1843 (4), 1625 (1.5), 1597 (1), 1537 (7), 1496 (1), 1468 (1), 1386 (1), 1360 (0.5), 1342 (1), 1226 (3), 1218 (2), 1176 (2), 1152 (1), 1115 (1), 1060 (2.5), 1038 (2), 1017 (1.5). IR (KBr, cm^{-1}): 2025 (10), 1990 (3), 1834 (6), 1624 (3), 1596 (2.5), 1535 (8), 1496 (2), 1432 (2), 1418 (0.5), 1386 (1), 1362 (1), 1342 (1.5), 1328 (1), 1282 (2), 1261 (1), 1224 (3.5), 1176 (3), 1149 (2), 1111 (2.5), 1082 (3.5), 1052 (3.5), 1015 (2), 860 (2), 783 (2), 733 (2.5), 687 (0.5), 660 (1), 637 (1), 515 (2.5). UV λ_{max} (ε/M^{-1} cm^{-1}) (CH$_2$Cl$_2$): 458 nm (49 300). UV λ_{max} (ε/M^{-1} cm^{-1}) (CH$_3$CN): 441 nm (57 700). Anal. Calc. for C$_{27}$H$_{21}$BF$_4$Fe$_2$O$_4$·0.1CH$_2$Cl$_2$: C, 52.75; H, 3.44. Found: C, 52.71; H, 3.44%.

4.10.3. [2-Methoxy-6-(CH=CH-μ-C–Fe$_2$(μ-CO)(η^5-C$_5$H$_5$)$_2$(CO)$_2$) naphthalene]$^+$ [BF$_4$]$^-$ (**15**)

As described in the procedure for Section 4.7, **1** (0.350 g, 0.8 mmol) was condensed with **12** (0.300 g, 1.6 mmol) to afford **15** as a red solid (0.295 g, 0.49 mmol) in 63% yield. ^{1}H-NMR (500 MHz, CD$_2$Cl$_2$): δ 10.13 (d, 1H, J = 14.6 Hz, μ-CCH=CH), 8.82 (1H, s, aryl), 8.22 (d, 1H, J = 14.6 Hz, μ-CCH=CH), 8.08 (1H, d, J = 8.3 Hz, aryl), 7.82 (d, 1H, J = 7.3 Hz, aryl), 7.66 (dd, 1H, J = 7.8, 7.3 Hz, aryl), 7.48 (d, 1H, J = 7.8, 7.3 Hz, aryl), 7.31 (s, 1H, aryl) 5.40 (s, 10H, C$_5$$H_5$), 4.16 (s, 3H, OCH$_3$). ^{13}C-NMR (126 MHz, CD$_2$Cl$_2$): δ 432.2 (μ-CCH=CH), 254.4 (μ-CO), 207.9 (^{t}CO), 162.3, 154.9, 151.7, 139.2, 139.1, 132.6, 129.9, 129.9, 129.3, 126.6, 121.0, 107.5, 92.2 (C_5H$_5$), 56.5 (OCH$_3$). IR (CH$_2$Cl$_2$, cm^{-1}): 2034 (9), 2005 (2), 1844 (4), 1621 (2), 1534 (10), 1497 (1), 1482 (1), 1397 (1), 1349 (3), 1195 (3), 1171 (7), 1154 (5), 1059 (3). IR (KBr, cm^{-1}): 2025 (9), 1994 (4.5), 1835 (5), 1620 (3), 1534 (10), 1496 (1), 1482 (1), 1419 (2), 1397 (1), 1349 (3), 1285 (2), 1264 (4), 1235 (2.5), 1194 (2.5), 1171 (8), 1084 (4), 1052 (3.5), 855 (1.5), 796 (1.5), 740 (1.5), 683 (1), 634 (1.5), 589 (1), 517 (1.5). UV λ_{max} (ε/M^{-1} cm^{-1}) (CH$_2$Cl$_2$): 511 nm (60 700). UV λ_{max} (ε/M^{-1} cm^{-1}) (CH$_3$CN): 481 nm (49 300). Anal. Calc. for C$_{27}$H$_{21}$BF$_4$Fe$_2$O$_4$·0.4CH$_2$Cl$_2$: C, 51.21; H, 3.40. Found: C, 51.22; H, 3.44%.

4.10.4. [2,2′-Dimethoxy-3-(CH=CH-μ-C–Fe$_2$(μ-CO)(η^5-C$_5$H$_5$)$_2$(CO)$_2$)-1,1′-binaphthalene]$^+$ [BF$_4$]$^-$ (**18**)

As detailed in the procedure for Section 4.7, **1** (0.114 g, 0.26 mmol) was condensed with **16** (0.20 g, 0.58 mmol) to afford **18** as a red solid (0.142 g, 0.19 mmol) in 73% yield. ^{1}H-NMR (500 MHz, CD$_2$Cl$_2$): δ 10.25 (d, 1H, J = 15.0 Hz, μ-CCH=CH), 9.12 (s, 1H, aryl), 8.28 (d, 1H, J = 8.0 Hz, aryl), 8.12 (d, 1H, J = 15.0 Hz, μ-CCH=CH), 8.07 (d, 1H, J = 9.0 Hz, aryl), 7.91 (d, 1H, J = 8.5 Hz, aryl), 7.50 (d, 1H, J = 10.0 Hz, aryl), 7.48 (m, 1H, aryl), 7.39 (ddd, 1H, J = 8.2, 6.5, 1.1 Hz, aryl), 7.37 (ddd, 1H, J = 8.7, 6.5, 1.1 Hz, aryl), 7.32 (ddd, 1H, J = 8.7, 6.5, 1.6 Hz, aryl), 7.19 (d, 1H, J = 8.7 Hz, aryl), 7.13 (d, 1H, J = 8.7 Hz, aryl), 5.40 (s, 5H, C$_5$$H_5$), 5.40 (s, 5H, C$_5$$H_5$), 3.83 (s, 3H, OC$H_3$), 3.50 (s, 3H, OC$H_3$). ^{13}C-NMR (126 MHz, CD$_2$Cl$_2$): δ 437.9 (μ-CCH=CH), 254.0 (μ-CO), 207.3 (^{t}CO), 156.2, 155.2, 153.4, 153.0, 148.9, 137.8, 134.4, 134.0, 131.5, 131.2, 130.7, 130.3, 129.4, 128.4, 127.4, 127.0, 126.7, 126.0, 125.1, 124.3, 118.1, 113.7, 92.0 (C_5H$_5$), 56.8 (OCH$_3$). IR (CH$_2$Cl$_2$, cm^{-1}): 2036 (10), 2005 (3), 1846 (4), 1618 (1), 1594 (1), 1570 (1), 1538 (7), 1511 (1), 1496 (2), 1377 (1), 1359 (1), 1221 (3), 1190 (1.5), 1107 (2), 1080 (3), 1056 (3). IR (KBr, cm^{-1}): 3113 (1), 2028 (10), 1994 (sh, 4), 1842 (5), 1618 (1), 1592 (1), 1538 (8), 1495 (2), 1458 (2), 1412 (2.5), 1358 (2), 1335 (1), 1269 (4), 1220 (4), 1150 (1), 1082 (5), 1047 (4.5), 858 (1), 801 (1), 755 (3), 690 (1), 659 (1), 602 (1), 598 (1), 540 (1), 514 (2). UV λ_{max} (ε/M^{-1} cm^{-1}) (CH$_2$Cl$_2$): 430 (26 200), 460 nm (24 700). UV λ_{max} (ε/M^{-1} cm^{-1}) (CH$_3$CN): 421 (24 300), 451 nm (sh, 22 400). Anal. Calc. for C$_{38}$H$_{29}$BF$_4$FeO$_5$·0.4CH$_2$Cl$_2$: C, 57.74; H, 3.73. Found: C, 57.83; H, 3.95%.

4.10.5. [2,2′-Dimethoxy-3-(E-2-(5-(E-2-(CH=CH-μ-C–Fe$_2$(μ-CO)(η^5-C$_5$H$_5$)$_2$(CO)$_2$))thienyl)ethenyl)-1,1′-binaphthalene]$^+$ [BF$_4$]$^-$ (**19**)

As described for the procedure in Section 4.7, **1** (0.066 g, 0.15 mmol) was condensed with **17** (0.110 g, 0.24 mmol) to afford **19** as a red solid (0.109 g, 0.12 mmol) in 80% yield. ^{1}H-NMR (500 MHz, CD$_2$Cl$_2$): δ 9.36 (d, 1H, J = 13.4 Hz, μ-CCH=CH), 8.26 (s, 1H, aryl), 8.25 (d, 1H, J = 12.7 Hz, μ-CCH=CH), 8.04 (d, 1H, J = 9.3 Hz, aryl), 7.94 (d, 1H, J = 14.4 Hz, aryl), 7.90 (d, 1H, J = 8.1 Hz, aryl), 7.85 (m, 1H, aryl), 7.76 (d, 1H, J = 15.9 Hz, CH=CH–thienyl), 7.58 (d, 1H, J = 15.9 Hz, CH=CH–thienyl), 7.49 (d, 1H, J = 9.0 Hz, aryl), 7.20–7.40 (m, 5H, aryl), 7.17 (d, 1H, J = 8.1 Hz, aryl), 7.11 (d, 1H, J = 8.3 Hz, aryl), 5.29 (s, 10H, C$_5$$H_5$), 3.82 (s, 3H, OC$H_3$), 3.45 (s, 3H, OC$H_3$). ^{13}C-NMR (126 MHz, CD$_2$Cl$_2$): δ 416.9 (μ-CCH=CH), 255.8 (μ-CO), 207.4 (^{t}CO), 158.7, 155.2, 154.7, 149.5, 146.0, 145.6, 138.9, 134.9, 134.2, 131.5, 131.1, 130.9, 130.3, 129.4, 129.3, 128.9, 128.3, 128.0, 127.4, 127.1, 126.2, 125.8, 125.7, 125.3, 124.0, 123.1, 118.9, 113.8, 91.4 (C_5H$_5$), 61.6 (OCH$_3$), 56.8 (OCH$_3$). IR (CH$_2$Cl$_2$, cm^{-1}): 2032 (7), 2002 (2), 1841

(4), 1583 (1), 1532 (10), 1495 (4), 1382 (3), 1370 (3), 1220 (4), 1176 (6), 1150 (2), 1113 (5), 1078 (4), 1059 (4). IR (KBr, cm^{-1}): 2021 (8), 1990 (4), 1832 (5), 1594 (1), 1531 (10), 1494 (4.5), 1433(6), 1371 (3), 1333 (2), 1264 (4), 1224 (6), 1176 (7), 1125 (4), 1083 (6), 1053 (5.5), 959 (1), 846 (1), 808 (1), 749 (1), 581 (1), 544 (1), 519 (1). UV λ_{max} (ε/M^{-1} cm^{-1}) (CH_2Cl_2): 608 nm (61 600). UV λ_{max} (ε/M^{-1} cm^{-1}) (CH_3CN): 566 (58 300) nm. Anal. Calc. for $C_{44}H_{33}BF_4Fe_2O_5S \cdot 2CH_2Cl_2$: C, 52.98; H, 3.55. Found: C, 53.59; H, 3.72%.

4.10.6. *[2,2′-Dimethoxy-3,3′-bis(E-CH=CH-μ-C–Fe₂(μ-CO)(η⁵-C₅H₅)₂(CO)₂)-1,1′-binaphthalene]⁺ ([BF₄]⁻)₂ (**21**)*

As detailed in the procedure in Section 4.7, **1** (1.00 g, 0.227 mmol) was condensed with **20a** (0.185 g, 0.50 mmol) to afford **21** as a red solid (0.443 g, 0.38 mmol) in 76% yield. ^{1}H-NMR (300 MHz, CD_2Cl_2): δ 10.26 (bm, 2H, μ-CC*H*=CH), 9.26 (s, 2H, aryl), 8.26 (bm, 2H, μ-CCH=C*H*), 8.14 (bd, 2H, aryl), 7.25–7.60 (bm, 6H, aryl), 5.51 (s, 20H, C_5H_5), 3.60 (s, 12H OCH_3). IR (CH_2Cl_2, cm^{-1}): 2034 (10), 1992 (5), 1844 (4), 1540 (5), 1361 (2), 1098 (4.5), 1080 (5), 1066 (5). IR (KBr, cm^{-1}): 2030 (9), 1993 (4), 1840 (4), 1543 (5), 1493 (1), 1476 (1), 1434 (2), 1414 (2), 1398 (1.5), 1337 (1), 1359 (1), 1300 (1), 1266 (2), 1226 (3), 1187 (1), 1104 (8), 1084 (10), 1071 (9), 1037 (10), 850 (1), 804 (1), 760 (1), 667 (1), 534 (2), 522 (2). UV λ_{max} (CH_2Cl_2): 453 nm. UV λ_{max} (CH_3CN): 446 nm. Anal. Calc. for $C_{54}H_{40}B_2F_4Fe_4O_8 \cdot 1.5H_2O$: C, 52.21; H, 3.46. Found: C, 52.29; H, 3.60%.

4.10.7. *[2,2′-Dimethoxy-6,6′-bis(E-CH=CH-μ-C–Fe₂(μ-CO)(η⁵-C₅H₅)₂(CO)₂)-1,1′-binaphthalene]⁺ ([BF₄]⁻)₂ (**22**)*

As detailed in the procedure in Section 4.7, **1** (1.00 g, 2.27 mmol) was condensed with **20b** (0.211 g, 0.57 mmol) to afford **22** as a red solid (0.489 g, 0.42 mmol) in 73% yield. ^{1}H-NMR (500 MHz, CD_2Cl_2): δ 9.99 (bm, 2H, μ-CC*H*=CH), 8.89 (bs, 2H, aryl), 8.37 (bm, 2H, μ-CCH=C*H*), 8.04 (bm, 4H, aryl), 7.79 (bs, 2H, aryl), 7.31 (bs, 2H, aryl), 5.45 (s, 20H, C_5H_5), 3.92 (s, 12H OCH_3). IR (CH_2Cl_2, cm^{-1}): 2034 (10), 2007 (sh, 5), 1842 (5), 1606 (7), 1531 (10), 1478 (1), 1380 (1.5), 1353 (2), 1221 (5.5), 1167 (6), 1094 (4), 1063 (5.5). IR (KBr, cm^{-1}): 2025 (9), 1991 (sh, 4.5), 1837 (5.5), 1613 (3), 1534 (10), 1478 (3), 1435 (1), 1381 (2), 1354 (3), 1282 (5), 1224 (6.5), 1169 (7), 1083 (5), 1056 (5), 974 (1), 857 (1), 824 (1), 804 (1), 741 (1), 703 (1), 640 (1.5), 520 (2). UV λ_{max} (ε/M^{-1} cm^{-1}) (CH_2Cl_2): 523 (52 000) nm. UV λ_{max} (ε/M^{-1} cm^{-1}) (CH_3CN): 496 (53 200) nm. Anal. Calc. for $C_{54}H_{40}B_2F_4Fe_4O_8$: C, 53.38; H, 3.29. Found: C, 53.59; H, 3.72%.

4.10.8. *[2,2′-Dimethoxy-6,6′-bis(E-2-(2-(5-(E-2-(CH=CH-μ-C–Fe₂(μ-CO)(η⁵-C₅H₅)₂(CO)₂))-thienyl)ethenyl)-1,1′-binaphthalene]⁺ ([BF₄]⁻)₂ (**26**)*

As summarised in the detailed procedure in Section 4.7, **1** (1.00 g, 2.27 mmol) was condensed with **25** (0.293 g, 0.50 mmol) to afford **26** as a red solid (0.548 g, 0.39 mmol) in 77% yield. ^{1}H-NMR (500 MHz, CD_2Cl_2): δ 9.45 (d, 2H, $J = 13.9$ Hz, μ-CC*H*=CH), 8.15 (d, 2H, $J = 4.2$ Hz, thienyl), 8.09 (d, 2H, $J = 8.8$ Hz, aryl), 8.07 (d, 2H, $J = 13.7$ Hz, μ-CCH=C*H*), 7.57 (d, 1H, $J = 16.1$ Hz, CH=C*H*–thienyl), 7.52–7.55 (m, 4H, aryl), 7.39 (d, 2H, $J = 15.9$ Hz, C*H*=CH–thienyl), 7.39 (d, 2H, $J = 3.9$ Hz, thienyl), 7.13 (d, 2H, $J = 9.0$ Hz, aryl) 5.33 (20H, s, Cp), 3.83 (s, 6H, OCH_3). ^{13}C-NMR (126 MHz, CD_2Cl_2): δ 415.8 (μ-*C*CH=CH), 255.3 (μ-CO), 208.0 (^{t}CO), 159.9, 157.1, 149.9, 146.2, 145.6, 139.0, 137.0, 135.3, 131.9, 131.2, 131.0, 130.4, 129.9, 126.7, 124.5, 121.2, 119.9, 115.2, 91.8 (Cp), 57.3 (O*C*H_3). IR (CH_2Cl_2, cm^{-1}): 2873 (1), 2031 (6), 2000 (2.5), 1840 (4), 1604 (2.5), 1538 (10), 1492 (3.5), 1384 (3.5), 1231 (5), 1170 (6.5), 1113 (5), 1058 (5). IR (KBr, cm^{-1}): 2019 (7), 1986 (sh, 4), 1830 (4), 1598 (2), 1530 (10), 1493 (4), 1432 (6), 1384 (3.5), 1371 (3.5), 1348 (2), 1339 (2), 1259 (4), 1227 (7), 1170 (8), 1113 (4), 1084 (5), 1054 (6), 950 (2), 844 (1), 798 (1), 639 (0.5), 580 (1), 548 (1), 518 (1.5), 484 (0.5). UV λ_{max} (ε/M^{-1} cm^{-1}) (CH_2Cl_2): 633 (75 400) nm. UV λ_{max} (ε/M^{-1} cm^{-1}) (CH_3CN): 594 (75 400) nm. Anal. Calc. for $C_{66}H_{48}B_2F_8Fe_4O_8S_2 \cdot 3CH_2Cl_2$: C, 49.14; H, 3.20. Found: C, 49.28; H, 3.55%.

4.11. *Crystal structure data for **1**, **9** and **15***

The crystalline samples of **1** were of very poor quality and grew as thin red lathes. Several specimens had the appearance of *plastic shavings*. Several attempts were made to obtain a crystal that diffracted satisfactorily prior to the selection of the sample reported. A small red crystal with dimensions 0.30 × 0.10 × 0.05 mm was *finally* chosen for data collection between 2.5 and 25° on θ at 123 K. The crystal hardly diffracted beyond 18° on θ. Compound **1** crystallises in the orthorhombic system. The space group is $P2_1nb$ or $Pmnb$. $P2_1nb$ was chosen (nonstandard setting of $Pna2_1$) and confirmed by the crystal structure analysis (repeated attempts to solve the structure in $Pmnb$ were unsuccessful). An absorption correction was applied and gave minimum and maximum transmission factors in the range 0.61–0.91. The structure was solved using direct methods in SHELXS-86 [38] and refined by full-matrix least-square techniques using SHELXL-97 [39]. The hydrogen atoms were treated as riding atoms with C–H distances in the range 0.93–0.98 Å [SHELXL-97 defaults]. It was evident at an intermediate stage of refinement {when $R[F^2 > 2\sigma(F^2)]$ was 0.20} that there were minor components of disorder associated with the $[BF_4]^-$ anion and a Cp ring. Coordinates for the minor sites of the $[BF_4]^-$ anion and Cp ring were generated and, for the final refinement cycles, soft DFIX and DELU/ISOR restraints were used in the SHELXL-97 calculations, [39]. The atoms of the major conformations of the $[BF_4]^-$ anion and (η^5-C_5H_5) ring were refined with anisotropic displacement parameters: the minor with isotropic displacement parameters to final site occupancies of 0.70(4)/0.30(4):0.87(4)/0.13(4) and 0.71(4)/0.29(4), respectively; disorder in a $[BF_4]^-$ anion is relatively common [40]. The final R-factor is 0.149 for 4218 observed reflections $[I > 2\sigma(I)]$ out of a total of 5564 measured reflections. However, the average intensity (σ) per reflection was 40(5) which is a good indication of poor crystal quality and diffraction. Compound **9** crystallises in the monoclinic system, space group $C2/c$. The data were analysed in a similar manner to that described above for **1**. The structure was solved using direct methods in SHELXS-97 [39] and refined by full-matrix least-square techniques using SHELXL-97 [39]. One of the methyl(C_5H_4) rings is disordered over two sites 0.75(1):0.25(1). The $[BF_4]^-$ anion is disordered over two sites 0.70/0.30 and disordered THF molecules with partial occupancy water molecules are also present in the lattice. Compound **15** crystallises in the monoclinic system, space group $P2_1/c$. The data were analysed and treated in a similar manner to **9**. Both of the (η^5-C_5H_5) rings are disordered over two different orientations which differ by rotation about the Fe...centroid axis with site occupancy factors of 0.52(4):0.48(4) and 0.59(3):0.41(3), respectively. The $[BF_4]^-$ anion is disordered over two orientations with occupancies of 0.62(2)/0.32(2).

5. Supplementary material

Crystallographic data for the structural analysis have been deposited with the Cambridge Crystallographic Data Centre, CCDC nos. 179433, 179434 and 179435 for compounds **1**, **9** and **15**. Copies of this information may be obtained free of charge from The Director, CCDC, 12 Union Road, Cambridge CB2 1EZ, UK (Fax: +44-1223-336033; e-mail: deposit@ccdc.cam.ac.uk or www: http://www.ccdc.cam.ac.uk).

Acknowledgements

Part of this work was supported by the EU under the TMR network CT-98-0166 and part was carried out under the auspices of COST D14 working group 0008/99. We also acknowledge the support of University College Dublin, the Belgium Government (IUAP IV/11), the fund for Scientific Research-Flanders (FWO G.0338.98;9.0407.98) and the University of Leuven (GOA 2000/03). J.F.G. thanks Dublin City University for the purchase of a P4 diffractometer. Elemental analyses were performed by Anne Connolly at University College Dublin.

References

[1] (a) N.J. Long, Angew. Chem. Int. Ed. Engl. 34 (1995) 21;
(b) T. Verbiest, S. Houbrechts, M. Kauranen, K. Clays, A. Persoons, J. Mater. Chem. 7 (1997) 2175;
(c) J. Heck, S. Dabek, T. Meyer-Friedrichsen, H. Wong, Coord. Chem. Rev. (1999) 1217;
(d) J.A. Mata, E. Peris, S. Uriel, R. Llusar, I. Asselberghs, A. Persoons, Polyhedron 20 (2001) 2083;
(e) A.M. McDonagh, M.P. Cifuentes, M.G. Humphrey, S. Houbrechts, J. Maes, A. Persoons, M. Samoc, B. Luther-Davies, J. Organomet. Chem. 610 (2001) 145;
(f) M.H. Garcia, J.C. Rodrigues, A.R. Dias, M.F.M. Piedade, M.T. Duarte, M.P. Robalo, N. Lopes, J. Organomet. Chem. 632 (2001) 133;
(g) M.H. Garcia, M.P. Robalo, A.P.S. Teixeira, A.R. Dias, M.F.M. Piedade, M.T. Duarte, J. Organomet. Chem. 632 (2001) 145.

[2] I.R. Whittall, A.M. McDonagh, M.G. Humphrey, Adv. Organomet. Chem. 42 (1998) 291.

[3] M. Nitay, W. Priester, M. Rosenblum, J. Am. Chem. Soc. 100 (1978) 3620.

[4] (a) C.P. Casey, M.S. Konings, R.E. Palermo, R.E. Colborn, J. Am. Chem. Soc. 107 (1985) 5296;
(b) C.P. Casey, M.S. Konings, S.R. Marder, J. Organomet. Chem. 345 (1988) 125.

[5] C.P. Casey, M.S. Konings, S.R. Marder, Y. Takezawa, J. Organomet. Chem. 358 (1988) 347.

[6] J.A. Bandy, H.E. Bunting, M.-H. Garcia, M.L. Green, S.R. Marder, M.E. Thompson, D. Bloor, P.V. Kolinsky, R.J. Jones, J.W. Perry, Polyhedron 11 (1992) 1429.

[7] (a) K. Clays, A. Persoons, Phys. Rev. Lett. 66 (1991) 2980;
(b) K. Clays, A. Persoons, Rev. Sci. Instrum. 6 (1992) 3285.

[8] (a) R.D.A. Hudson, I. Asselberghs, K. Clays, L.P. Cuffe, J.F. Gallagher, A.R. Manning, A. Persoons, K. Wostyn, J. Organomet. Chem. 637–639 (2001) 435;
(b) R.D.A. Hudson, A.R. Manning, D. Nolan, I. Asselberghs, R.V. Boxel, A. Persoons, J.F. Gallagher, J. Organomet. Chem. 619 (2001) 141;
(c) T. Farrell, T. Meyer-Friedrichsen, J. Heck, A.R. Manning, Organometallics 19 (2000) 3410.

[9] (a) J. Zyss, J.-F. Nicoud, J. Coquillay, Chem. Phys. 8 (1984) 4160;
(b) J.L. Oudar, R.J. Hierle, Appl. Phys. 48 (1977) 2699.

[10] S.K. Kurtz, T.T. Perry, J. Appl. Phys. 39 (1968) 3798.

[11] M.L. Green, S.R. Marder, M.E. Thompson, J.A. Bandy, D. Bloor, P.V. Kolinsky, R.J. Jones, Nature 330 (1987) 360.

[12] (a) A. Togni, G. Rihs, Organometallics 12 (1993) 3368;
(b) G.G.A. Balavoine, J.-C. Daran, G. Iftime, P.G. Lacroix, E. Manoury, J.A. Delaire, I. Maltey-Fanton, K. Nakatani, S. Di Bella, Organometallics 18 (1999) 21;
(c) G. Iftime, G.G.A. Balavoine, J.-C. Daran, P.G. Lacroix, E. Manoury, C. R. Acad. Sci. Paris Serie 11c Chimie/Chemistry 3 (2000) 139;
(d) A. Klys, J. Zakrzewski, K. Nakatani, J.A. Delaire, Inorg. Chem. Commun. 4 (2001) 205.

[13] S.R. Marder, J.W. Perry, W.P. Schaefer, B.G. Tiemann, Organometallics 10 (1991) 1896.

[14] (a) R. Andreu, I. Malfant, P.G. Lacroix, H. Gornitzka, Chem. Mater. 11 (1999) 840;

(b) F. Steybe, F. Effenberger, U. Gubler, C. Bosshard, P. Günter, Tetrahedron 54 (1998) 8469;
(c) F. Steybe, F. Effenberger, S. Beckmann, P. Krämer, C. Glania, R. Wortmann, Chem. Phys. 317 (1997) 317;
(d) P.G. Lacroix, K. Nakatani, Adv. Mater. 9 (1997) 1105.

[15] (a) J. Roncali, Annu. Rep. Prog. Chem. Sect. C 95 (1999) 47;
(b) J. Roncali, Chem. Rev. 97 (1997) 173 (and references therein).

[16] (a) V.P. Rao, A.K.-Y. Jen, K.Y. Wong, K.J. Drost, Tetrahedron Lett. 34 (1993) 1747;
(b) C. Maertens, C. Detrembleur, P. Dubois, R. Jérôme, C. Boutton, A. Persoons, T. Kogej, J.L. Brédas, Chem. Eur. J. 5 (1999) 369;
(c) F. Würthner, C. Thalacker, R. Matschiner, K. Lukaszuk, R. Wortmann, J. Chem. Soc. Chem. Commun. (1998) 1739.

[17] D. Prim, G. Kirsch, J.-F. Nicoud, Synlett (1998) 383.

[18] (a) H. Seeboth, S. Andreae, Z. Chem. 16 (1977) 399;
(b) E.H. Elandaloussi, P. Frère, P. Richomme, J. Orduna, J. Garin, J. Roncali, J. Am. Chem. Soc. 119 (1997) 10774.

[19] (a) E. Hendrickx, C. Boutton, K. Clays, A. Persoons, S. Van Es, T. Biemans, B. Meijer, Chem. Phys. Lett. 27 (1997) 241;
(b) A. Gussoni, G. Zerbi, J.J.G.S. Van Es, H.A.M. Biemans, E.W. Meijer, Synth. Met. 80 (1996) 201.

[20] J.J.G.S. Van Es, A.M. Biemans, E.W. Meijer, Tetrahedron: Asymmetry 8 (1997) 1825.

[21] K. Ding, Y. Wang, L. Zhang, Y. Wu, Tetrahedron 52 (1995) 1005.

[22] D. Cai, D.L. Hughes, T.R. Verhoeven, P.J. Rieder, Tetrahedron Lett. 36 (1995) 7991.

[23] J. March, Advanced Organic Chemistry, 4th ed., Wiley, New York, 1992, p. 242.

[24] (a) N. Bloembergen, Y.R. Shen, Phys. Rev. 133 (1964) 37;
(b) J.L. Oudar, D.S. Chemla, J. Chem. Phys. 66 (1976) 2664.

[25] (a) M.S. Paley, J.M. Harris, H. Looser, J.C. Baumert, G.C. Bjorklund, D. Jundt, R.T. Twieg, J. Org. Chem. 54 (1989) 3774;
(b) F. Effenberger, F. Würthner, Angew. Chem. Int. Ed. Engl. 32 (1993) 719;
(c) S.L. Gilat, S.H. Kawai, J.-M. Lehn, J. Chem. Soc. Chem. Commun. (1993) 1439;
(d) S.L. Gilat, S.H. Kawai, J.-M. Lehn, Chem. Eur. J. 1 (1995) 275.

[26] (a) W.P. Schaefer, J.M. Spotts, S.R. Marder, Acta Crystallogr. Sect. C 48 (1992) 811;
(b) C.P. Casey, M.S. Konings, S.R. Marder, Polyhedron 7 (1988) 881;
(c) C.P. Casey, M.S. Konings, R.E. Palermo, R.E. Colborn, J. Am. Chem. Soc. 107 (1985) 5296.

[27] R.E. Colborn, D.L. Davies, A.F. Dyke, A. Endesfelder, S.A.R. Knox, A.G. Orpen, D. Plaas, J. Chem. Soc. Dalton Trans. (1983) 2661.

[28] J. March, Advanced Organic Chemistry, 4th ed., Wiley, New York, 1992, p. 19.

[29] F. Würthner, S. Yao, J. Schilling, R. Wortmann, M. Redi-Abshiro, E. Mecher, F. Gallego-Gomez, K. Meerholz, J. Am. Chem. Soc. 123 (2001) 2810.

[30] For crystallographic data on guinoniod dihydrothiophene-2,5-diylidenes see: (a) K. Takahashi, T. Suzuki, K. Akiyama, Y. Ikegami, Y. Fukazawa, J. Am. Chem. Soc. 113 (1991) 4576;
(b) G. Hieber, M. Hanack, K. Wurst, J. Strähle, J. Chem. Ber. 124 (1991) 1597.

[31] For crystallographic data on oligothiophenes see: F. Van Bolhuis, H. Wynberg, E.E. Havinga, E.W. Meijer, E.G. Starring, J. Synth. Met. 30 (1989) 381.

[32] G. Bruno, F. Nicoló, A. Rotondo, R. Gitto, M. Zappalá, Acta Crystallogr. Sect. C 57 (2001) 1225.

[33] J.F. Gallagher, K. Hanlon, J. Howarth, Acta Crystallogr. Sect. C 57 (2001) 1410.

[34] F.A. Allen, O. Kennard, Chem. Des. Autom. News 8 (1993) 1, 31.

[35] K. Roque, F. Barangé, G.G.A. Balavoine, J.-C. Daran, P.G. Lacroix, E. Manoury, J. Organomet. Chem. 637–639 (2001) 531.

[36] (a) M.C.B. Colbert, J. Lewis, N.J. Long, P.R. Raithby, D.A. Bloor, G.H. Cross, J. Organomet. Chem. 531 (1997) 183;
(b) A. Houlton, J.R. Miller, J. Silver, N. Jasim, M.J. Ahmet, T.L. Axon, D. Bloor, G.H. Cross, Inorg. Chim. Acta 205 (1993) 67;
(c) A. Houlton, N. Jasim, R.M.G. Roberts, J. Silver, D. Cunningham, P. McArdle, T. Higgins, J. Chem. Soc. Dalton Trans. (1992) 2235;
(d) B.J. Coe, C.J. Jones, J.A. McCleverty, D. Bloor, P.V. Kolinsky, R.J. Jones, J. Chem. Soc. Chem. Commun. (1989) 1485.

[37] P.G. Lacroix, K. Nakatani, Adv. Mater. 9 (1997) 1105.

[38] G.M. Sheldrick, Acta Crystallogr. Sect. A 46 (1990) 467.

[39] G.M. Sheldrick, SHELXS-97 and SHELXL-97, University of Göttingen, 1997.

[40] J.F. Gallagher, E.C. Alyea, G. Ferguson, X. Zheng, Acta Crystallogr. Sect. C 50 (1994) 16.